Transient conductivity in poly-LED devices

van de Logt, L.M.A.

Award date:
1996

Transient conductivity in Poly-LED devices.

Author :Leon van de Logt.

Author: Leon van de Logt.

Supervisors: Dr. Ir. P. Blom
Prof. Dr. J. Wolter.

Title: Transient conductivity in Poly-LED-devices.

Abstract

From steady-state current-voltage measurements it has been observed that the conduction of holes in a polymer LED is dominated by space charge effects, whereas the electron conduction is severely limited by traps. In order to investigate the trapping effects photocondution experiments has been performed. It appears that the photocurrent of holes exhibit an extremely slow response after switching the light on and off. Due to this slow response a modulation technique which is commonly used for studying photoconduction, is not suited for determining the absolute value of the spectral photoconductivity. We observed that the hole photocurrent transients are only weakly dependent on the exciting wavelenght varying from 600nm to 2000nm. The current transients are also observed when charge carriers are injected from the contacts into the polymer. From these measurements it appeared that trapping is about 5% in hole-only devices while the trapping in electron-only devices is about one order of magnitude. Furthermore, it is demonstrated that the electrical history plays a vital role in the amount of trapping in electron-only devices.

A model is proposed in which trapping and detrapping of charge carriers is responsible for the transients. The current relaxation in hole-only devices is qualitatively in good agreement with the proposed model. An exponential density of states with a typical width of 700 K is derived from this model. The response of electron-only devices seems to resemble the predictions of a more dedicated random walk theory for hopping conduction. Applying this theory we observed that the density of states for the traps is also exponential with a typical width of 800 K.

Contents.

1. Introduction

Today, LED-devices are very common in our daily life. The active material is mostly made of an inorganic material such as $GaAs1_{1-x}P_x$. Since it was discovered in 1990 that some conjugated polymers can also be used for light emitting purposes, a lot of research has been done to improve the performance of these light emitting devices. Today, an external quantum efficiency of 2 % has been reached. At Philips Research the soluble polymer OC_1OC_{10}PPV is used which has very good luminescent properties. At an operating voltage of 3 V and a current of 5 mA/cm^2 a radiance of 100 Cd/m^2 is achieved which is comparable to the radiance of a computer monitor.

Polymers have some major advantages above the commonly used inorganic materials. The processing of these devices is in general very cheap and the mechanical properties are promising (they are flexible and light). By changing the chemical composition somewhat, one can easily obtain different colors. Of special interest for Philips Electronics N.V. is the application in large area thin film LEDs and the usage as back light for displays.

A major problem in polymer LEDs is their short operating lifetimes which also decreases with brightness level. The light emission comes from the recombination of electron and holes in the bulk of the polymer. It has been proposed[5] that the device characteristics pf a PLED are determined by the contact. However, recent experiments[12] showed that the steady-state current density-voltage (J-V) characteristics on PPV devices are bulk limited and controlled by trapping effects. It has been observed that electrons, in contrast to holes, are severely trapped which results in unbalanced electron and hole transport. To investigate the trapping kinetics in PPV devices, transient (photo) currents have been measured for both electrons and holes. In order to optimize the light emission of polymer LEDs, a balanced charge injection and charge transport should be achieved. Therefore, understanding in the fundamental properties of PPV is crucial for the optimization of a polymer LED.

In this study the transport properties of the polymer and especially the trapping and detrapping of charge from traps will be discussed. This has been done by measuring the transient current in hole-only devices as well as electron-only devices. These transients are initiated due to illumination of the device and by switching the voltage on or off.

In order to measure the photocurrent, a modulation technique based on a lock-in amplifier was used. It appeared that the photocurrent is very sensitive to variations in the chopping frequency indicating that steady-state is not reached. Direct measurement of the current reveals interesting features. From the current-time characteristic it follows that the relaxation of the hole-current under illumination towards an equilibrium is very slow (in the order of minutes). The slow relaxation in PPV has already been found by Lee et al[15] for photonenergies above the bandgap. They proposed an explanation based on a diffusion mechanism of bipolarons towards the surface of their device. However, in our configuration such a diffusion mechanism seems not very obvious. In this report a model is proposed based on a semiconductor band model where trapping and detrapping of charge carriers from traps is responsible for the transients.

Because Calcium contacts, which are used for electron-only devices, oxidize very fast, these devices had to be measured in a nitrogen box. Unfortunately, it was not possible to perform photoconduction experiments in an inert atmosphere. However, with a voltage step the same sort of transients are observed and it appears that the trapping effect in electron-only devices is much larger compared to hole-only devices. For the electron-only devices, hopping transport seems to be a more appropriate theory to fit the transients.

Support for the hopping theory comes from the temperature measurements on these devices. In this report the amount of trapping as a function of the temperature is illustrated for both hole-only and electron-only devices. The temperature measurements on the electron-only devices are in good agreement with the predictions of the hopping theory.

2. Theory of the polymer LED

§ 2.1 Introduction

In this chapter the electrical characterization of the Polymer LED (PLED) will be discussed. First a brief description of the conduction mechanisms in a conjugated poymer will be given Then a model describing the device characteristics of a PLED is proposed. Finally, various mechanisms for photoconduction and their corresponding time dependence will be discussed.

§ 2.2 Electrical conduction in conjugated polymers.

The polymer that is used for the polymer LED is called poly (p-phenylene vinylene) (PPV) and is a π-conjugated polymer shown in the picture below. This means that the polymer has a string of alternating single (σ-bond) and double (σ- and π-bond) bonds in his chains. Such a conjugated polymer can be regarded as a semiconductor where the conduction is along the

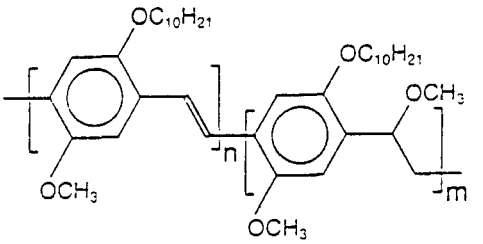

Fig.2.1 Chemical structure of the soluble OC_1OC_{10} poly (dialkoxy-p-phenylene vinylene) (PPV).

one-dimensional chains. The fact that a conjugated polymer is conducting as well as the excistence of a band gap find their origin in the Peirels theorem[1,2].

If the π-bonds in the conjugated polymer would be broken, the polymer could be regared as an one-dimensional lattice with one unbonded electron per lattice-site. So in this case we would have a one-dimensional metal with a half-filled band. However, the Peierls theorem states that an one-dimensional metal with a half-filled band is unstable. Electron-phonon interactions will distort the lattice, thus the unit cel will be doubled and an energy gap will appear at the Fermi-level. This is the basis for a semiconductor model and is shown below. The spacing between succesive lattice-sites is modulated. The distortion then leads to pairing

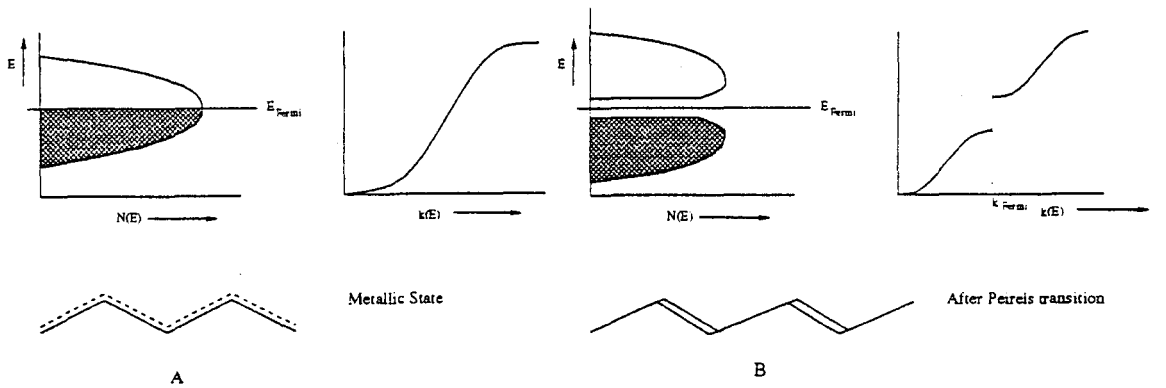

Fig 2.2 Schematic view of the changes in the density of electronic states and the molecular structure before and after the Peierls ttransition.

of succesive sites along the chain, or dimerization. The chain of monomers can be dimerized in two distinct patterns as is shown in figure 2.3 for polyacetylene. If all monomers are

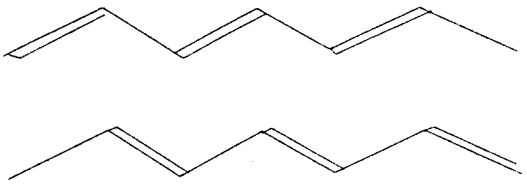

Fig. 2.3 The two different conjugated phases of polyacetylene or dimerisation.

equivalent, the energies of the two binding structures are equal. The conduction properties of a dimerized semiconductor are theoretically derived in terms of a semiconductor band picture using single-chain one-electron models based upon the Su-Schieffer-Heeger hamiltonian[3]. The conduction properties then arise from collective excitations of the polymer chains. In contrast to convential semiconductors the conjugated polymers exhibit a new type of excitations, a domain wall or soliton separating regions of different bonding, as schematically indicated in figure 2.4. A soliton can be charged (0,+ or - depending on the electron occupation) and is able to move since the variation of the system energy as the soliton moves is small. In a non

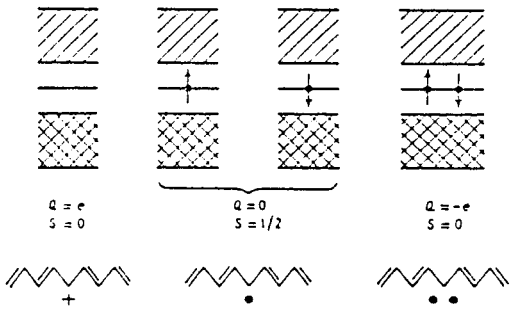

Fig 2.4 Schematic view of a) positively charged soliton with zero spin b) neutral soliton with spin ½ c) negatively charged soliton with zero spin.

degenerate system as for example PPV the lowest excited state, which is now called a polaron, consists of two solitons. The second soliton converts the chain back to the energetically most favourable state. The two solitons, of which a polaron consists, are bound together as a molecule, and the corresponding energy states are therefore no longer midgap but move to the valence band and the conduction band. Bipolarons are pairs of polarons. A polaron is captured in the potential minimum of the other. Polarons and solitons are in the band model principally localized states. Thus following the semiconductor model, the addition of an electron or hole to a conducting polymer results in a self-localized excitation which has deformed the semiconductor lattice.

However, the applicabilities of the semiconductor model has seriously been challenged due to the results of spectroscopic studies[26]. In contrast to the theoretical band model, the chains in a polymer are not infinitely long and the conjugation is often broken due to defects,

kinks, and disorder. Thus in practice a polymer chain consists of conjugated parts separated by non conducting parts. The real question is now how strong the conjugated parts of a polymer chain are coupled. For strong coupling the semiconductor band model holds, whereas for weak coupling the conjugated segments behave as individual molecules. Especially, in strongly disordered systems the variations in the environment of the indivdual sites give rise to a large spreading in the site energies, which reduces the coupling strenght. Which model, the semiconductor band model or the molecular exciton model, is more suited for the description of the electrical and optical properties of conjugated polymers is still a subject of ongoing research. In the present study we use a simple view of a conduction and valence band, with electrons and holes. However, the charge carriers have a very low mobility which reflects their localization on the conjugated segments of the chain.

§ 2.3 Band structure in polymer LEDs.

The starting-point of our theory is a semiconductor model for the polymer. In figure 2.5 a schematic band diagram of a PLED is shown.

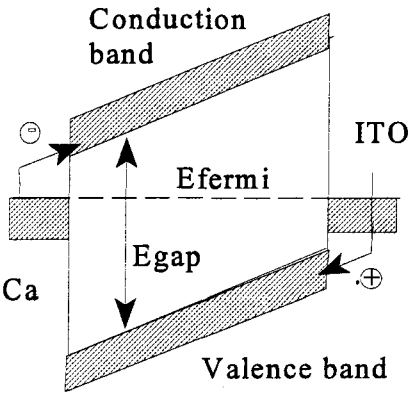

Fig. 2.5 Schematic view of a PLED with electron and hole injecting contacts.

A polymer LED exists of a polymer layer sandwiched between two different metal contacts. The bottom contact is an Indium Tin Oxide contact (ITO) with a high work function close to the valence band. The top contact is evaporated Calcium with a low work function close to the conduction band of the PPV. ITO serves as a hole injecting contact and Calcium as the electron injecting contact. In thermal equilibrium the Fermi level should be equal in all materials. Therefore, at zero bias, the Fermi level is equal in both metals resulting in a built in voltage as can be seen in figure 2.5. The difference in work function causes an internal electric field. Under positive bias the Fermi level of the negative contact (Ca) is lifted upwards. In this case the internal field is lowered until this field is totally compensated by a specific bias. This bias is called the flatband potential or the built in voltage as shown in figure 2.6A. In this situation there is only diffusion current due to the difference in Fermi level. A higher bias gives a forward current illustrated by 2.6B. From this picture it is shown that a PLED is a diode because in reverse the injection of electrons from the ITO into the conduction band is not possible due to the high barrier which is nearly equal to the bandgap of 2.0 eV. The same

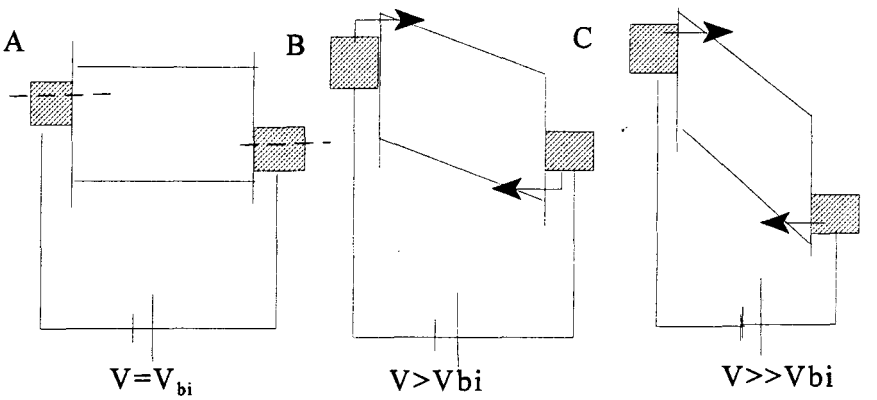

Fig. 2.6 Schematic illustration of the built in voltage. A gives a PLED at the built-in voltage and B gives a picture of a PLED under forward bias. In this case both contacts can inject carriers. C shows the Fowler-Nordheim tunneling under forward bias of the PLED..

holds for the injection of holes from the Ca contacts into the valence band. Figure 2.6C gives the bandstructure of a PPV LED under forward bias where the injection of charge carriers is illustrated as a tunneling process. In this case the current of the PLED is contact limited and is described by Fowler-Nordheim tunneling. The injection of carriers and therefore the current is determined by the barrierheight Φ_B. This injection process is a generally accepted model although recent experiments[12] showed that the current is controlled by space charge in the polymer. The influence of space charge on the current will be discussed now.

§ 2.4 Electrical description under steady-state.

This paragraph considers the electrical behavior of an one-carrier polymer LED. Since each injected carrier contributes one excess charge to the polymer, space charge plays a vital role, via the Poisson equation, in the behavior of all one-carrier injection currents. In steady state, the carrier flow is governed by ohms law and the Poisson equation [13,16]. These are given by:

$$J(x) = q\mu n(x)E(x)$$
$$\frac{\varepsilon}{q}\frac{\partial E(x)}{\partial x} = [n(x)-n_0]+[n_t(x)-n_{t,0}] \qquad (2.1)$$

with:

- n(x) the total free carrier density.
- n_0 the thermally generated density of free carriers.
- n_t (x) the total trapped carrier density.
- $n_{t,0}$ the thermal equilibrium of n_t (x).
- ε the static dielectric constant.
- μ the carrier mobility.
- E(x) the electric field.
- J(x) the current density.

These equations are the most general forms for our model. To describe the effects of trapping quantitatively, two other equations are needed which introduce time dependent effects. In the next paragraph, the Poisson equation and ohms law will be used for the derivation of the current -voltage characteristics. After that, the trapping in polymer LEDs will be discussed.

§ 2.4.1 Hole-only devices under steady-state.

In order to study the conduction properties of holes, an ITO contact is used as bottom electrode and an evaporated Au contact as top electrode. In these, so called, hole-only devices the work function of both electrodes are close to the valence band of PPV, preventing electron injection. This is schematically shown by figure 2.7.
A typical example of the current density-voltage characteristic is given by figure 2.8. As can be seen the current is quadratic in the voltage. This behavior is characteristic for space charge

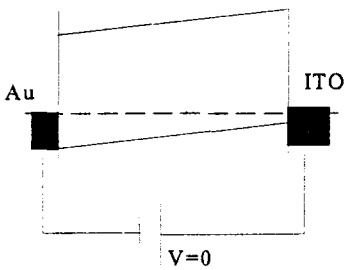

Fig.2.7 Schematic view of a hole-only device under zero bias.

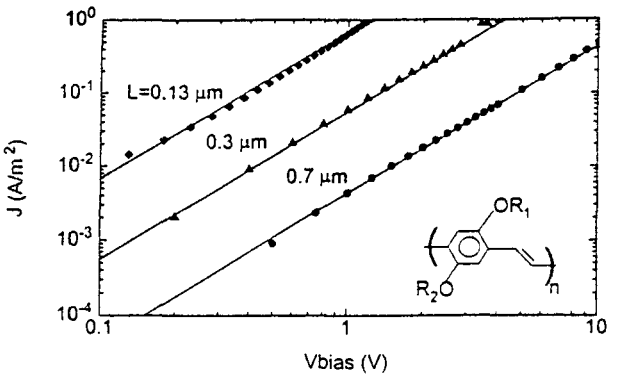

Fig.2.8 Experimental and calculated (solid lines) J-V characterisitcs of a hole-only device.

limited current (SCLC). The absence of a sharp increase in the current (trap filled limit)[13] indicates that the hole transport in our PPV can be regarded as trap free.

For the trap free case, the last part on the right hand side of equation 2.1 can be ignored. If the injection barrier is low, which is in a good approximation true, we can take E(0) = 0 as the boundary condition. For simplicity, we will use this condition further.

In the regional approximation method[16], the Poisson equation can be separated in two parts for n(x) and n_0. n(x) decreases monotonically from a high value near the injecting electrode to a low value near the collecting electrode crossing the value n_0 at some place in the polymer. This crossing point depends on the current J as schematically indicated in figure 2.9. Because n(x) is not constant near the injecting electrode and $n(x) >> n_0$, the electric field will

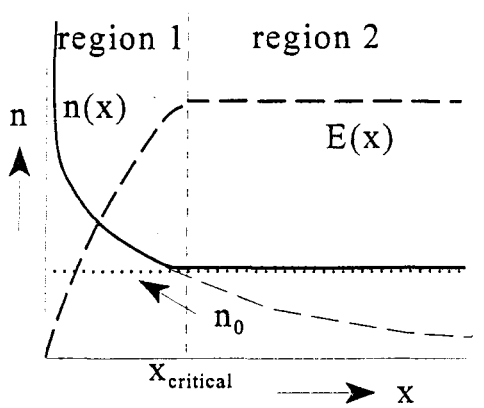

Fig. 2.9 Separation of the LED in two regions. The electrode is at x=0. Region 1 is the SCLC regime and region 2 is the ohmical regime.

also depend on x. It follows from Poisson's equation that dE/dx ~ n(x). In the first region the field will rise and in the second region where n_0>>n(x) the field will be a constant. Above the critical voltage, the injected space charge dominates in the whole device and region2 is not present anymore. The current is space charge limited (SCL) in the whole polymer and E becomes a function of the distance in the whole device. From ohms law and Poisson's equation we find a differential equation for the space charge limited current [8,12] (SCLC):

$$\frac{\partial E}{\partial x} = \frac{J}{\mu \varepsilon E} \tag{2.2}$$

Integration gives:

$$E(x) = \sqrt{E^2(0) + \frac{2Jx}{\mu \varepsilon}} \tag{2.3}$$

If E(0)=0, as is for an ohmic contact we obtain the relation for the space charge limited current as:

$$J = \frac{9}{8}\varepsilon_0 \varepsilon_r \mu \frac{V^2}{L^3} \tag{2.4}$$

This IV characteristic is observed for hole-only devices in the whole voltage range. It is clear from the above that the current in hole-only devices is determined by space charge effects in the polymer and is therefore bulk limited.

§ 2.4.2 Electron-only devices under steady-state.

For electron-only devices two Calcium contacts are used with have work functions close the conduction band of the polymer which makes electron injection easy. The bandstructure in these devices is schematically shown in figure 2.10. Figure 2.11 shows a typical current density-voltage characteristic of an electron-only device. These devices shows an abrupt transition from an ohmical behavior to a space charge limited current. It is expected that this transition towards a SCL current is caused by trapping in the bulk of the polymer. Returning to

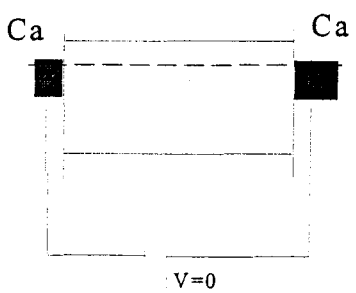

Fig.2.10 Schematic view of a electron-only device under zero bias.

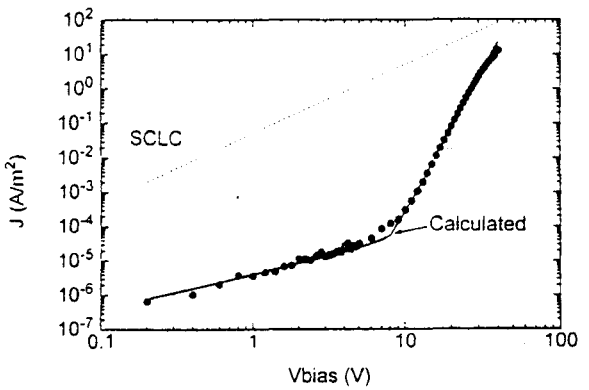

Fig.2.11 Experimental and theoretical (solid line) J-V characteristicof an electron-only device.

figure 2.9 we have for the second region $n(x)=n_0$ and this may appropriately be called an ohmic region because E is a constant (dE/dx=0). The first region is dominated by space charge and is not ohmic.

Below a critical current, the field E is independent of the distance in nearly the whole polymer. This gives rise to the familiar ohms law where E is constant:

$$J = n_0 q \mu \frac{V}{L} \tag{2.5}$$

In this case, region 1 can be neglected which is the case for electron-only devices in the low voltage regime as can be seen from figure 2.11.

If traps are included the right term in formula 2.1 is also used. This problem is really not different from the one shown by figure 2.9. The only difference is that we have a more or less abrupt transition from the ohmic to the SCLC regime due to the filling of traps. For trap levels located at a single energy the current directly switches to the SCLC. The transition is extremely sharp then. The more gradual increase in fig.2.11 points to a distribution of trap level energies. For low currents the SCL region breaks up into two subregions. In the first region n(x) dominates and in the second region $n_t(x)$ dominates. The third region is the ohmic region.

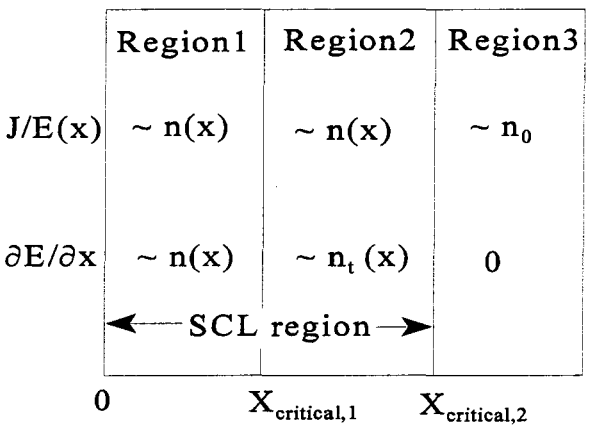

Fig. 2.12 Schematic illustration of the separation of the LED in three regions when trapping is included. In the first region n(x) dominates and in the second region n_t (x) dominates. The third region is the ohmical regime.

This three region problem is schematically illustrated by figure 2.12. The reason for this separation into three regions is that the injected carriers "fill" the initially empty traps as soon as they are sufficient in number to compete with the thermal carriers. For low injection, the current is therefore ohmic (equation 2.5) because all the injected charge is trapped and space charge can not be build up. Above a critical voltage a large part of the traps are filled and therefore space charge is build up. This can be seen in the J-V characteristic as an abrupt increase in the current. For higher injection the traps will soon be filled (trap filled limit: TFL) and the current can not increase further due to the filling of traps. The current is now fully space charge limited and is desribed by formula 2.4. Figure 2.13 below gives an illustration of this filling of traps.

The intermediate regime gives the transition from ohmic to space charge current and is a

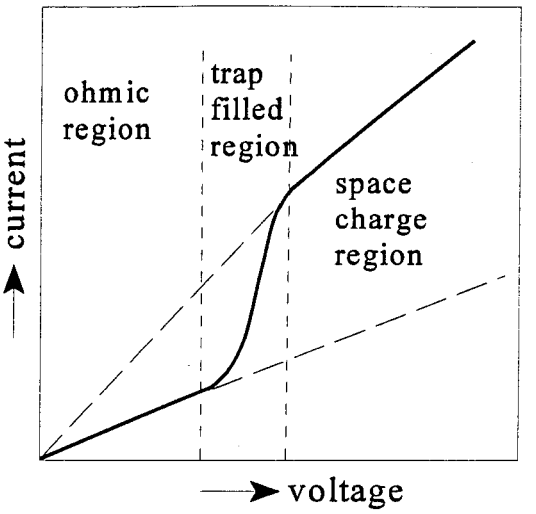

Fig. 2.13 Schematic representation of the I-V characteristic when traps are included. Three regions exists now.

simple extension to the description given before. For a single set of trap level energies the increase in the current is very abrupt. For a distribution of trap level energies, which is more probable for a disordered system as PPV, the transition to the SCLC regime is more gradual. Experiments shows that this distribution of traps is exponential in PPV [12] given by:

$$N_{trap} = \frac{N_t}{k_b T_0} \exp\left(-\frac{(E_c - E_t)}{k_b T_0}\right) \tag{2.6}$$

Here, N_{trap} is the density of traps at the trap energy E_t . T_0 represents the typical width of the trapping regime. This trap distribution implies for the intermediate regime (trap filled limit region) the following IV characteristic[16].

$$J = N_c q \mu_n \left(\frac{\epsilon_0 \epsilon_r}{q N_t}\right)^r \frac{V^{r+1}}{L^{2r+1}} C(r) \tag{2.7}$$

With $r=T_0/T$ and N_c the density of states in the conduction band. From this theory it follows that the current in electron devices is trap limited.

§ 2.5 Injection mechanisms.

So far it is demonstrated that both the electron and hole current are controlled by the conduction properties. As a result the injection barriers are too small to play any significant role in the conduction properties. In order to estimate the effect of an injection barrier, we compare the injection and bulk limited currents without traps. For the current injection into low mobility semiconductors as PPV, where diffussion effects must be taken into account, it is assumed that thermionic emission-diffusion theory [4] is applicable. This is given by the next formula:

$$J = q N_c \mu E(0) e^{\left(-\frac{q\phi_B}{kT}\right)} \tag{2.8}$$

N_c is the effective density of states in the conduction or valence band. The barrierheight ϕ_B is

lowered by the image force effect known as the Schottky-effect.

As mentioned in §2.3 an another injection process is the tunneling of carriers through the injection barrier. This is a quantummechanical effect where the carrier has the possibility to penetrate the barrier. Parker [5] proposed that the I-V characterisics of polymer LEDs are controlled by this injection mechanism. This tunnel current in PPV is given by Fowler-Nordheim [5,6,7] tunneling:

$$J \propto E_0^2 \exp(-\frac{\kappa}{E_0}) \tag{2.9}$$

For a triangular barrier, κ is given by [4] :

$$\kappa = \frac{8\pi\sqrt{2m^*}\,\phi_B^{3/2}}{3qh} \tag{2.10}$$

In fig.2.14 the contact limited current of equation 2.8 and 2.9 are shown together with the bulk limited current of equation 2.4. It appears that for low bias the current is diffusion limited whereas for high bias the current is SCL. For Φ_B<0.2eV the current is given by 2.4 in the whole bias regime and this is found in the experiments of figure 2.8 [12]. These calculations

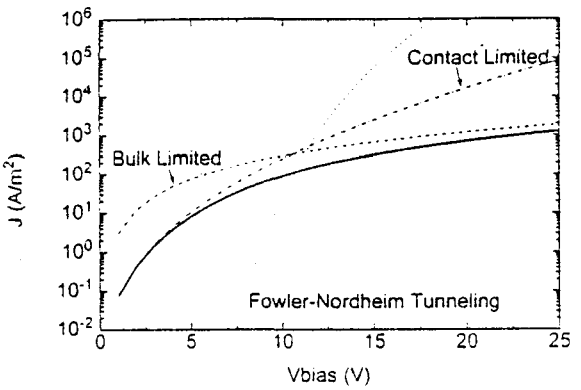

Fig. 2.14 Calculated I-V characteristic (solid line) for a PPV LED. The bulk limited (SCLC) as well as the diffussion limited injection and the Fowler-Nordheim current, assuming E=V/L are included.

shows that quantitatively at these high fields the Fowler-Nordheim tunneling exceed the experimentally observed current. The importance of the observation of space charge limited current in our hole-only devices is that it demonstrates that the hole current is bulk limited and not injection limited as proposed by Parker[5].

It is of crucial importance to understand whether the device characteristics and performance are controlled by the trapping in the polymer. For further investigations on trapping in electron and hole conduction, photoconduction experiments are a good candidate. Furthermore, the influence of different contacts on the photoconduction can be investigated.

§ 2.6 Photoconduction mechanisms.

In §2.4 a description of the bandstructure of the polymer LED has been given together with

some injection mechanisms in §2.5. In the present section, the properties of photogenerated charge carriers and the underlying mechanisms in order to investigate trapping will be discussed.

In polymers there are several possible mechanisms for photoconduction. These mechanisms have been more extensively studied in organic molecular crystals such as anthracene. So, in this sense care should be taken to use these concepts for polymers but many indications show that the mechanisms in polymers are closely related to molecular crystals. As the picture below shows, there are three important mechanisms for photogeneration of carriers.

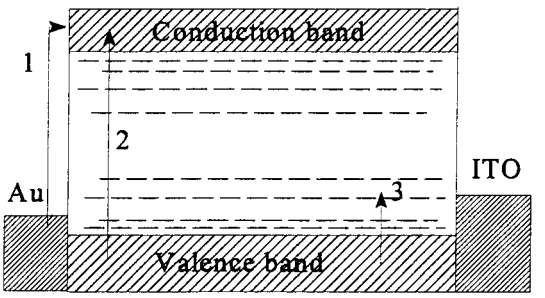

1) photo-injection over the Schottky-barrier.
2) Band-to-band photoconduction.
3) Photo detrapping of trapped charge.

Fig. 2.15 Mechanisms for photoconduction in a hole-only device.

The first mechanism is the generation of photocarriers via photoemission from electrodes and is the most interesting mechanism for investigations on injection limited currents. This process is called internal photo emission (IPE) and is an important mechanism for investigating injection limited currents. From this mechanism we can determine the work function of the metal since the possibility for photogeneration is dependent on the barrier height. Different metals have different workfunction and dependent on the number of surface states there is a difference in barrier height. In a spectral photocurrent measurement this can be observed. We introduce the quantity Quantum Yield (QY) defined as the total number of carriers per photon. The QY is thus a measure for the normalized photocurrent. From calculations [8,9,10] it follows that for wide bands the square root of the QY should be proportional with the photonenergy; $QY^{1/2} \sim E_{photon}$. For narrow bands the QY itself should proportional with the photonenergy; $QY \sim E_{photon}$. The barrierheight can than be determined by extrapolating the data to zero QY. For the same electrode we can also determine the barrier lowering (Schottky effect) since this dependends on the voltage. At higher voltage the barrier is lowered and therefore the extrapolation to zero QY should depend on the voltage.

The second mechanism is the intrinsic photoconduction process. Here, a photon with an energy larger than the bandgap ($E_{photon} > E_{gap}$) is needed to create an electron-hole pair which can contribute to the conduction. From this measurement we can directly determine the energy gap of the polymer. Some research has already been done on these high photon energies. In PPV a bandgap of ± 2,1 eV is found. It should be noted that it is also possible to direct excite the ground state of the singlet excitation. In this case the photon generates an exciton which is something like a bounded electron-hole pair. Due to an external applied field, this exciton, which is a neutral particle that doesn't contribute to the conduction, can dissociate to

produce a free electron and a hole. The dissociation needs more energy which can come from exciton-surface interactions. Whether the formation of excitons actually happens is still under discussion so we will pay no further attention to this exciton mechanism.

The third mechanism is optical detrapping of trapped charge and plays an important role in investigations on bulk limited currents. For this mechanism we need relatively low photon energies ($E_{photon} < E_{gap}$). This process can give some information about the purity of the polymer. The impurities and physical defects (traps) result in electronic states below the first excited state of the pure polymer. Carriers can be trapped in these states and can also be optically detrapped with low photon energy as shown in figure 2.15. Because trapping in a hole-only device is small according to figure 2.8 a small photoconduction current is expected for these devices. Electron-only devices are controlled by trapping in the polymer and therefore large photoconduction effects are to be expected. However, the investigations on traps is very complicated because of time dependence as well as the electrical history of the sample. The population will vary from day to day and from sample to sample, so obtaining reproducible results is very difficult. Furthermore, the photocurrent due to detrapping of trapped charge is generally very small because the density of traps is much smaller than the density of states of the conduction- or valence band. Special techniques are often required to measure these photocurrents well.

From the above discussion we can see that for our polymer samples only the third mechanism needs low photon energies. We can use this for our determinaton of traps in the polymer to overcome too complicated situations. By using low energies the other mechanisms can be excluded (also the exciton case) from the photoconduction experiment and investigations on bulk limited currrents can be carried out.

§ 2.7 Current relaxation towards equilibrium.

As stated in paragraph 2.4, two extra equations have to be added to the semiconductor model in order to describe the time dependent effects in the conduction due to trapping. Taking the system out of equilibrium results in a transient current due to trapping. The perturbation may arise from a strong absorbed light pulse or a voltage step. Let us first start with the simple case of one discrete trap level where the distribution of free carriers is the same for every x. The dynamical behavior of the traps is described with a Fermi-Dirac distribution and semiconductor physics. The time dependent flow of mobile carriers in the presence of traps is now characterized by the following equations[16] :

$$
\begin{aligned}
J(x.t) &= q\mu n(x,t)E(x,t) + \frac{q}{V}\frac{\partial E(x,t)}{\partial t} \\
\frac{\partial J_c(x.t)}{\partial x} &= -q\left[\frac{\partial n(x,t)}{\partial t} + \frac{\partial n_t(x,t)}{\partial t}\right] \qquad (2.11) \\
\frac{\varepsilon}{q}\frac{\partial E(x,t)}{\partial x} &= [n(x,t) - n_0] + [n_t(x,t) - n_{t,0}]
\end{aligned}
$$

The first equation consist of two terms; the first is the conduction current $J_c(x,t)$ and the second is the displacement current. The diffusive contribution to the conduction current is omitted in order to make the analysis not too complicated. Furthermore, equation 2.11 has

become time dependent. The trapping kinetics of a single traplevel are described as:

$$\frac{dn_t}{dt} = \frac{n}{\tau_{capture}} - \frac{n_t}{\tau_{escape}} \tag{2.12}$$

Here, n is the free carrier concentration , n_t is the trapped carrier concentration. Approximate solutions for an insulating crystal characterized by slow trapping has already been worked out by Many et al[16]. The solutions are obtained for traps situated at one trap level and the density of the trapped charge always small compared to the unoccupied sites. From these solutions it follows that even in a space charge limited system, J(t) decays approximately exponentially.

For the simple case of one trap level and the presence of slow trapping as in our case ($\tau_{trapping} >> \tau_{transit}$) we have a quasi stationary behavior, with J(t) and n(t) decaying slowly with time. The displacement current $\partial E(t)/\partial t$ in formula 2.11 can be neglected now. In PPV LEDs the absorbtion coefficient for the used wavelenghts is low and therefore it is assumed that the excitation is homogenous in the whole bulk of the polymer. The change in the conduction current $\partial J_c(t)/\partial x$ in the second equation of formula 2.11 can be omitted now. Furthermore the electric field is taken constant (E=V/L) and space charge effects are omitted in first instance. In 2.12, $\tau_{esc.}$ is the carrier release (escape) time which is for a semiconductor band model given by:

$$\frac{1}{\tau_{escape}} = \nu_{phonon} \exp -\left(\frac{E_c - E_t}{k_b T}\right) \tag{2.13}$$

where E_c is the energy of the conduction band and E_t the energy of the trap level. The absolute temperature is given by T. ν_{phonon} is the attempt to escape frequency and has a maximum value of about 10^{13} Hz, equal to the maximum frequency for crystal vibrations. An important remark to equation 2.13 is that this formula holds for a pure semiconductor band model. A polymer is not a pure semiconductor and it is expected that hopping transport is an important transport mechanism in polymers. The prefactor in the escape time is then changed. This will be discussed later. It is assumed that the carrier capture time or trapping time τ_{cap} is given by:

$$\tau_{capture} = \frac{1}{(N_t - n_t)C} \tag{2.14}$$

In 2.14, N_t is the total number of trapping sites, C is a constant that can be determined from the equilibrium situation. Formula 2.14 states that when all traps are occupied, there is no capture anymore which is of course true and is therefore a reasonable assumption. From 2.13 we can see that deep traps immobilize carriers longer than shallow traps. In contrast to Many et al[16] we shall not assume that the trapped charge is always small compared to the unoccupied sites. In hole-only devices the amount of traps is small compared to the free carriers according to the J-V characteristics and the traps are almost completely occupied. The capture time shall therefore not be constant.

The second equation of 2.11 is a particle conservation equation. Without a charge carrier gradient in the x-direction, $dJ_c/dx=0$ and the equations states that the loss of free carriers is equal to the amount of the trapped carriers. In a steady-state situation (as described in §2.3) we have for the thermal equilibrium value of the trapped carriers:

$$n_{t0} = N_t \exp -\left(\frac{E_t - E_f}{k_b T}\right) = \frac{N_t}{1 + N/n_0} \tag{2.15}$$

With $N=N_c\exp(-(E_c-E_t)/kT)$. The latter expression in 2.15 is another way of writing the Fermi-Dirac expressions and is a more convenient one which we will use.
In steady-state the capture and release of carriers is also in equilibrium and we have:

$$\frac{dn_t}{dt} = \frac{n_0}{\tau_{capture}} - \frac{n_{t0}}{\tau_{release}} = 0 \quad \Leftrightarrow \quad \frac{n_0}{n_{t0}} = \frac{\tau_{capture}}{\tau_{release}} \tag{2.16}$$

where the subscript 0 refers to the equilibrium concentration of the trapped and free carriers. The free carrier concentration is given by $n_0=N_c\exp(-(E_c-E_F)/kT)$ as follows from the familiar semiconductor statistics. From the equilibrium condition and 2.15 it follows that $C=1/(N\tau_{esc})$.

From equation 2.12 we see that we have normal (one exponential) relaxation if we take the capture and release times as constant (an one order differential equation). In a more realistic situation this is not true. Because $\tau_{capture}$ varies with the total number of trapped charge, which increases as time progress, the capture time will also increase and, hence, the relaxation is slower than in the beginning. So the relaxation can turn from an exponential decay in the beginning to a non-exponential relaxation with a long tail as time progress.

To do some calculation with these formulas we need to know some quantities. If we know the Fermi level, n_{t0} follows from formula 2.15. Via the equilibrium condition 2.16 we know the capture time in equilibrium and C is determined from 2.14. The model given here for one trap level can be extended to a multiple trapping case where we take an exponential distribution in energy for the traps. In this case a set of trapping equations (formula 2.12) should be solved which can be done numerically (see appendix A). The equilibrium values for a given Fermi level should be calculated then for every trap level independently.

An extension to the model can be made by adding the gradient in the conduction current. As mentioned before we assumed dJ_c/dx to be zero, that is, there is no gradient in the current flow in the x-direction. If a conduction current is included in the trapping model, the particle conservation law (second equation of 2.11) is then maintained in his original form. This means that the amount of lost free carriers per unit time is not only reduced by the amount of the trapped carriers but also by the carriers that flows to another position in the polymer. This conduction current may change the relaxation because the amount of free carriers can be different on different places in the polymer. The dynamical behavior of the traps is still described by the formulas given above but the amount of free carriers is now different for every place and time. For this extension to the model a program is also written and is given in appendix B.

§ 2.8. Dispersive transport and random walk theory.

In the past many photoconduction experiments have been done on a wide variety of disordered materials[14,24]. From these experiments it was illustrated that the transient current showed a remarkable relaxation towards equilibrium. Instead of the normal exponential or Gaussian relaxation one found a current trace with a slow, long tail. A typical example of this non-exponential behavior is given in figure 2.16. The tranport of carriers and the time relaxation of

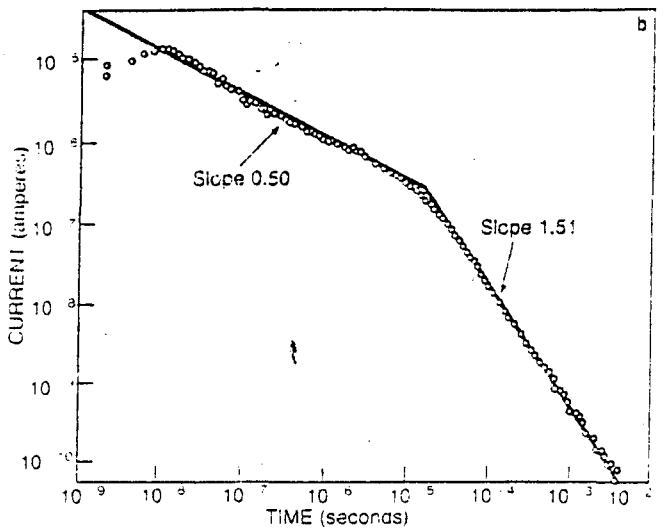

Fig 2.16 Log-log plot for intrinsic hydrogenated amorphous silicon a-Si:H at 160K. The current decays algebraically over nearly six decades of observation time of the experiment. (Adapted from T.Tiedje, 1984).

the current involved will be discussed now.

Transport in a disordered material occurs via a sequence of charge-transfer steps from one localized site to another in the presence of an applied electric field. If the transfer step involves thermal activation from the site to the conduction band in which the charge diffuses to the next site, the process is called trapping. Tunneling directly between sites is known as hopping. Fig 2.17 shows these processes schematically. Due to disorder, the transfer time between two

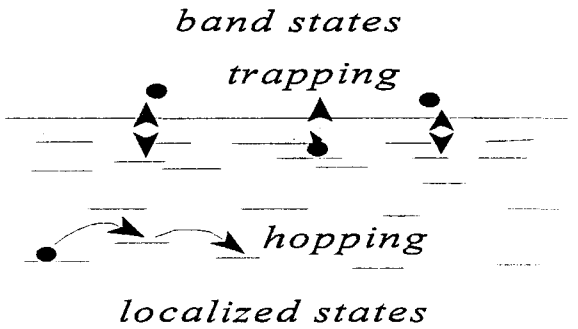

Fig 2.17 Illustration of band transport with trapping and hopping transitions between localized states in the energy gap.

sites can be a random variable characterized by the probability $\psi(t)dt$ that the time for an individual event is between t and t+dt. The transport and relaxation in disordered solids is now called "dispersive " when the mean waiting time between these events diverges[14]. This variation in time is the key for the observed peculiar features of the current traces I(t) in disordered materials. The perturbation which brings the system out of equilibrium can be due to photoexcitation or by a voltage pulse. By specifying the probability distribution $\psi(t)$ and the spatial bias introduced by the electric field, one can calculate the properties of a packet of charge propagating across a sample. The random walk theory assumes that each charge carrier

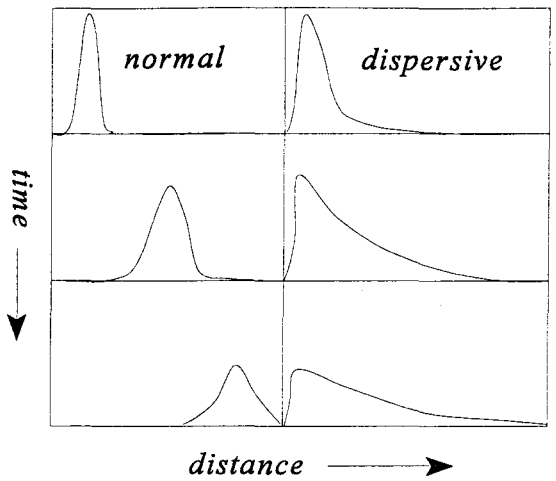

Fig. 2.18 transiting packet of charge in time for normal and dispersive transport.

undergoes a random walk biased in a preferred direction by the applied voltage. The propagating packet of charge depends entirely on the probability distribution $\psi(t)$. The current trace of figure 2.16 can now be understood in terms of this random walk theory assuming that:

$$\psi(t) \sim t^{-(1+\beta)} \tag{2.17}$$

From this probability distribution we can have normal (Gaussian) or dispersive transport [14] for $\beta<1$ as shown by fig 2.18. We see that with increasing time, the peak remains at the initial position, while the mean is continuously displaced from it. This unusual behavior originates in the relatively small, but finite, probability of an event time that is much larger than a typical one. These rare, but long event times can have a large effect on carrier motion. The probability distribution of formula 2.17 gives the space averaged conduction current traces described by the following formula:

$$\begin{aligned} I(t) &= t^{-(1-\beta)}, \qquad t<t_r \\ I(t) &= t^{-(1+\beta)}, \qquad t>t_r \end{aligned} \tag{2.18}$$

The cross-over between the two formulas is at the transit time t_r. A double logaritmhic plot of the current trace of formula 2.18 is simply two straight lines where the sum of the slopes is -2 independent of the value β. With these formulas the current trace of figure 2.16 can be explained in terms of dispersive transport and this random walk theory.

Hopping involves the tunneling of an electron between localized states. The tunneling rate is a sensitive function of the distance and energy separation between these states. The site-to-site variation in these quantities as a result of disorder can result in a tunneling-rate spectrum, which generates the dispersion. The formulas describing the time dependence of the current in the case of hopping will be discussed in the following paragraph.

Another way of introducing disorder in a material is by including localized electronic states that act as traps. Traps promotes a spectrum of intrinsic times that limits the transport. In the case of extensive multiple trapping, the total time spent in traps far exceeds the total transit

time in the conduction band. Often, one takes an exponential distribution for the traps with a typical width T_0. The dynamics of a multiple trapping regime is already discussed in paragraph 2.6 in terms of semiconductor physics.

In conclusion we can say that dispersive transport originates from the probability distribution when the mean waiting time between events diverges. This dispersion can be introduced by the disorder in the material and is either controlled by trapping or by hopping. A main question is whether this random walk theory as derived for disordered systems is also applicable in explaining the transient effects in conjugated polymers.

§ 2.8.1 Hopping conductivity far from equilibrium.

From paragaph 2.8 it was illustrated that dispersive transport is not only introduced by trapping and detrapping of charge carriers, but also by hopping of charge carriers between localized sites. In this paragraph we will focus our attention on this hopping conductivity in the non-equilibrium situation. Because of the energetic and spatial disorder of the polymer we will give only a simple and general model of these dynamics[1].

Once again a multiple trapping regime is used where traps are defined as states in which carriers are temporarily immobilized reducing the effective mobility. Hopping can occur when the distance between the sites and the energy difference is not too large.

Two formulas completely determines the dynamics of the hopping carriers in a multiple trapping regime. One describes the hopping-rate which gives the rate of hopping as a function of energy difference and spatial difference between sites. The other is the density of states (DOS) of the band tail states as used in the semiconductor model. These formulas are:

$$\begin{aligned} \nu_{if} &= \nu_0 \exp\left(\frac{-2R_{if}}{a}\right)\cdot\exp\left[-\frac{(E_f - E_i)}{kT}\right], \qquad (E_f > E_i) \\ g(E) &= \frac{N_L}{kT_0}\exp\left(\frac{E}{kT_0}\right) \end{aligned} \tag{2.19}$$

The first equation gives the hopping rate. R_{if} is the distance between the initial and final sites. ν_0 is a constant which is of the order of the phonon frequencies (10^{12} - 10^{13} Hz), a is the localization or wavefunction radius which is important for the overlap between sites and can be estimated to 10Å. The absolute temperature is presented by T and k_b is Boltzmann's constant. E_f and E_i represents the final and initial energy of the hopping carrier. This formula can be compared with the escape time from the semiconductor model (formula 2.13). The main difference is in the prefactor which has become an exponential function instead of the phononfrequency alone. The second equation is similar to formula 2.6.

In summary, 2.19 states that a carrier starts at an initial energy E_i and will hop to a final energy E_f with a certain chance for this hopping process. Because the occupation is different for different energies, the chance of hopping is also controlled by the DOS. If we want to know the typical hopping rate of a particular carrier at a given energy, the hoppingrate has to be multiplied with the DOS. This typical hopping rate is found from formula 2.19 as:

$$\nu_{typical} = \frac{1}{\tau_s}\exp\left(-\frac{E_t - E_i}{kT}\right) \tag{2.20}$$

Here, τ_s is a specific time constant and E_t is the most probable final energy. This energy depends on the temperature and is close to the conduction band edge often denoted by the mobility edge which separates the fast sites from the slow sites. This is illustrated in the following picture. In this view, a demarcation energy $E_d(t)$ can be defined as the energy where

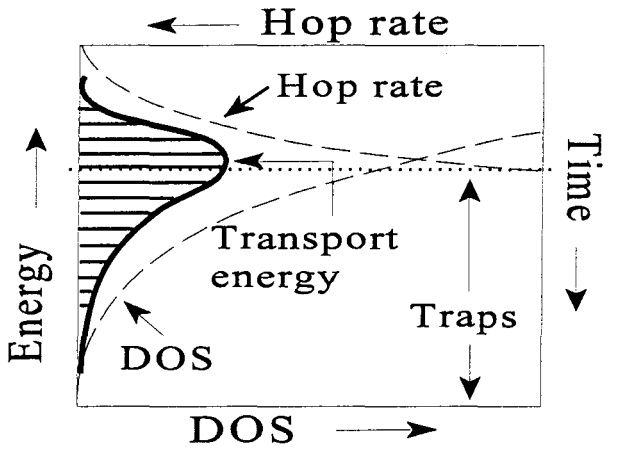

Fig.2.19 Schematic view of the existence of a most probable energy resulting from the hopping rate and the DOS. As time progress the top will move to lower energies indicating the demarcation level.

a typical hopping rate is comparable with the experimental timescale. Carriers on sites that are lower than the demarcation energy have less chance of escaping from this site than carriers above this energy. This demarcation energy E_d (t) is the energy level where the rate is 1/t and is more or less a kind of pointer that points to the energy level "where the action is". This means that at longer times, E_d (t) comes deeper in the band tail because these states have a slower response. Therefore, hopping introduces dispersive transport which is clearly illustrated by the time variation in the demarcation energy level.

This demarcation level can be calculated from the formula for $\nu_{typical}$ leading to:

$$E_d(T,t) = E_t(T) - kT\ln\left(\frac{t}{\tau_s}\right) \tag{2.21}$$

with τ_s a specific time constant separating the traps from the conducting sites. From this formula we can see that E_d changes slower for longer times as expected because "the action" is at the deep trap levels.

The current can also be determined now. For the determination of this current, the fraction of carriers at time t is calculated and the current is described by:

$$I(t) = (const.)\frac{\nu_0 a^2}{k_b T_0/e}\left(\frac{T_0}{T}\right)^2 (\nu_0 t)^{-1+\frac{T}{T_0}} \tag{2.22}$$

When the carriers are in the transportstates, they drift with a field dependent mobility μ_0 (as follows from SCLC discussed in §2) until they are trapped again in traps below E_d.

So far this theory is a simple model in that it doesn't account for interaction effects between carriers. These interactions makes the theory a lot more difficult but introduces some

important features in the model. For example, they introduce dynamical correlations in the time evolution which can be sequential or simultaneous correlations. The long time relaxation will be even longer now than the theory predicts. Furthermore, the discussion about the existence of dispersive transport has been split into the dynamics of trapping and the dynamics of hopping. In a real polymer, however, it is not unlikely that these two processes coexist.

3. Experimental

§ 3.1 Introduction

In this chapter the experimental setup will be discussed wich is used for the measurements. The first section gives a short description of how the PPV devices are made. Then it will be explained how the intended measuring technique works and in the next chapter the problems, using this technique on an PPV sample, will be the subject of discussion. For further properties of the setup the reader is referred to the literature [8].

§ 3.2 Structure and fabrication of the sample.

The samples were made on a 3x3 cm glass substrate. Four LED devices can be made on this glass via a mask. Because the light of the LED is going through the glass the contact on the glass should be transparent. This is also important for our measurements because we want to photoexcite the polymer. An Indium-Tin-Oxide (ITO) contact is used for this purpose. On this contact, a polymer film is made with a spin-coating technique that gives a relatively homogeneous thickness of the soluble polymer on the glass. This is done by putting a drop of the polymer on the glass and placing it on a rotating disc. Dependent on the viscosity of the polymer and the rotation speed of the disc, a film will be generated with a predetermined thickness. The polymer chains are now distributed in a random way. The second contact is evaporated onto this polymer film. We used hole-only and electron-only samples. In the first case a gold contact is used together with an ITO contact and in the second case two Calcium contacts are used. A schematic view of a complete (hole-only) sample is given below.

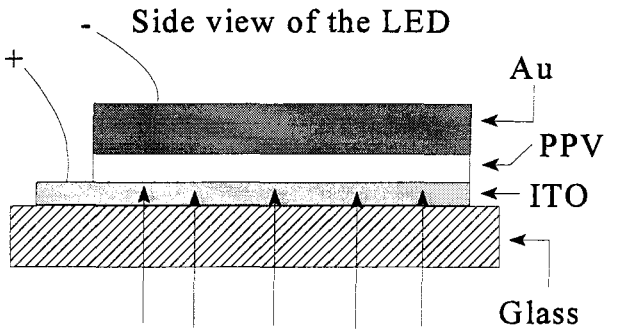

Fig. 3.1 Structure of the sample.

§ 3.3 Experimental setup.

The setup is primarily meant for the measurement of the normalized photocurrent but the computer programme is equipped with several other measurement methods. The total system is shown in picture 3.2. As can be seen, the main part of the setup exists of a lamp, some filters to get the right wavelenght, focussing lenses and the sample. The setup is controlled by

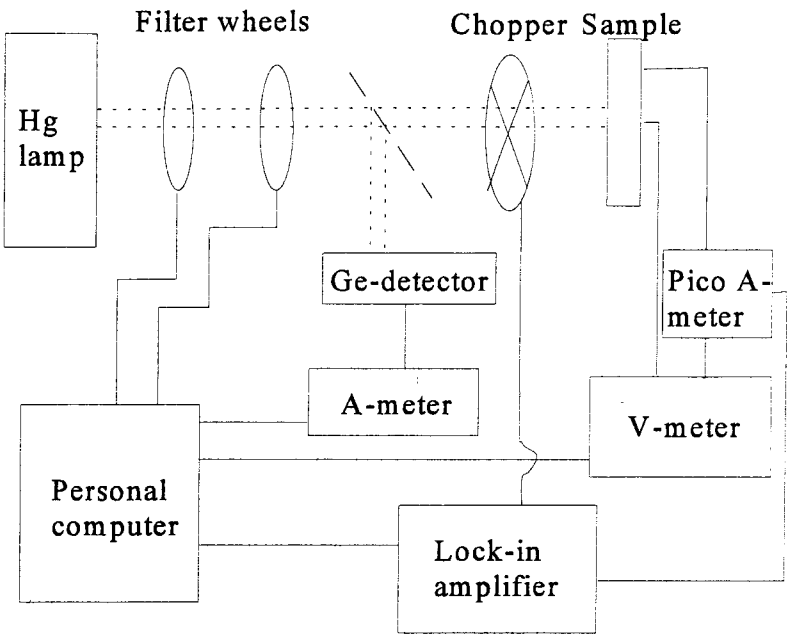

Fig. 3.2 Schematic view of the experimental setup. The dotted line represents the light. Several lenses were used between the Hg lamp and the sample to obtain a small spot on the sample.

a computer. For the light we used a 100 Watt mercury lamp which is mounted in a Oriel lamp housing (model 60100). The lamp is connected to a power supply with pre-ignition for the lamp (Oriel 68806). To avoid destruction of the lamp due to its own heating in the housing, the lamp is watercooled with a recirculating cooling system (Oriel 60200). The light from this housing can be focussed on the filterwheels. We use two filter wheels; one with blocking filters and one with interfering filters. With these two filter wheels one can generate monochromated light within a precision of 5 nm. To get the right wavelenght, the wheels are driven by a stepping motor which is on his turn controlled by the computer. The first filter wheel also has a non-transmitting site so that we can "turn of the light" with the computer.

After the monochromating part the light is split off by a semi-tranparent mirror and the light intensity of the reflected part is measured with a germanium detector and a Keithley 485 autoranging picoampèremeter. This splitting of the light is necessary because we want to measure the *normalized* photocurrent from the sample and so we have to know the monochromated light intensity. As the spectrum of a mercury lamp and the filters varies a lot in intensity, measurement of this intensity is very important. The whole experimental setup is calibrated for this purpose. However, in this calibration an undetermined wavelenght dependence can still exist. This is due to a wavelenght dependence of the mirror and the lenses resulting in different focussing areas onto the sample. The total number of photons on the sample can be determined from the detector readout and the various calibrations. In formula:

$$n_{sample} = \frac{Cal_{setup} \cdot I_{detector}(A)}{Cal_{Ger.-detector}(A/W) \cdot E_{photon}(J)} \qquad (3.1)$$

The dimension of each function is placed between brackets and the word "Cal" is reserved for the various calibrations.

To get the Quantum Yield we have to divide the measured photocurrent by this $n(\lambda)$. To be able to measure this very small photocurrent we use a modulation technique. By chopping the light with a mechanical chopper we can modulate the light that falls on the sample. With a lock-in ampliflier (an EG&G 5206) the small currents generated by the light can be measured. The reference comes from the mechanical chopper as a 1 Volt square signal. The LIA gets the measuring signal from a current sensitive preamplifier (an EG&G 181) which is connected between the voltage source and the sample. This amplifier gives a voltage on his output that is proportional to the current. To the sample a bias can be applied with a programmable voltage source (Keithley 230) which is also controlled by the computer.

With the above description of the experimental setup the QY can be measured. The program allows us to make several other measurements like the current-voltage characteristic or the current-time characteristic. For these two we measure the current directly with the Keithley 485 picoampèremeter instead of the lock-in. Measuring the *photo*current in this way is difficult because of the small currents. For the exact details of the calibration methods and the programme, the reader is referred to the literature [8].

4. Results and discussion.

§4.1 Analysis of the experimental setup.

By choosing a low chopping frequency, the transit time of the carriers becomes smaller then the time constant of the chopper. We used a chopping frequency of 40 Hz which is equal to $2{,}5*10^{-2}$ s. When we estimate the drift time of the carriers as:

$$\tau = \frac{d^2}{V\mu} \tag{4.1}$$

we find for V=4Volt, d=3000Å and $\mu \approx 0{,}5*10^{-10}$ m^2/Vs [12] a transit time of $\tau \approx 4.5*10^{-4}$ s. This means that the light is turned on and off with a time interval equal to the chopping time which is significantly longer than the transit time. So, in this point of view the carriers have more than enough time to reach the other side of the polymer and steady-state is supposed.

In figure 4.1 the dependence of the QY on the wavelenght of the incident light is shown at various chopping frequencies.
It is observed that the QY depends heavily on the frequency in the whole range of chopping-

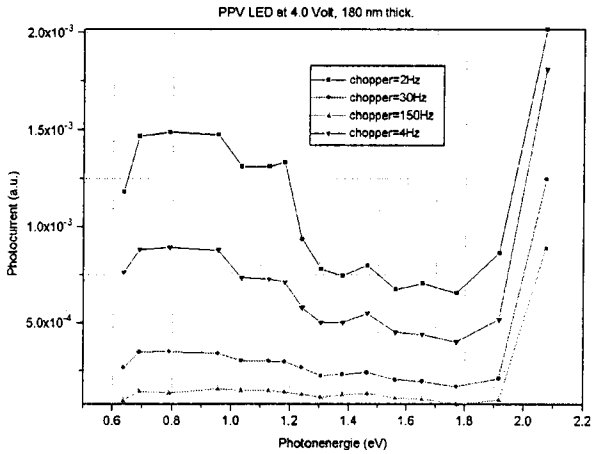

Fig.4.1 Normalized photocurrent (QY) as a function of the photonenergy of the incident light at different chopfrequencies.

frequencies. This means that steady-state is not reached within the timescale of the chopping-frequencies. We used choppingfrequencies from 1 to 200 Hz. Even at 1 Hz (this is a time interval of 1 s !!) steady-state was not reached. At this low frequencies technical problems also occur. The signal to noise ratio (S/N) of the lock-in [11] becomes large at these low frequencies so the measurement at 1 Hz is troublesome. The lock-in also takes a longer time to reach a steady value because of its averaging procedure over all the chopping cycles.

The very small photocurrent can also be measured with the Keithley 485 picoamperemeter instead of the lock-in. Unfortunately, the accuracy of this direct measurement of the photocurrent is less than with the lock-in (this is, of course, also the primary reason why we wanted to

use a lock-in technique). The absolute value of the photocurrent can now be determined by subtracting the (in general) steady background current. Figure 4.2 shows some of these transient current measurements on the same sample in the long time regime (15 to 30 minutes of measuring time) at two different photonenergies and two voltages. From this figure it can be seen that the photocurrent has a very slow response. Depending on the wavelenght the current takes at least 5 to 10 minutes or even more to reach a steady state.

The question rises what this means for our QY measurement. Apparently formula 4.1 is not

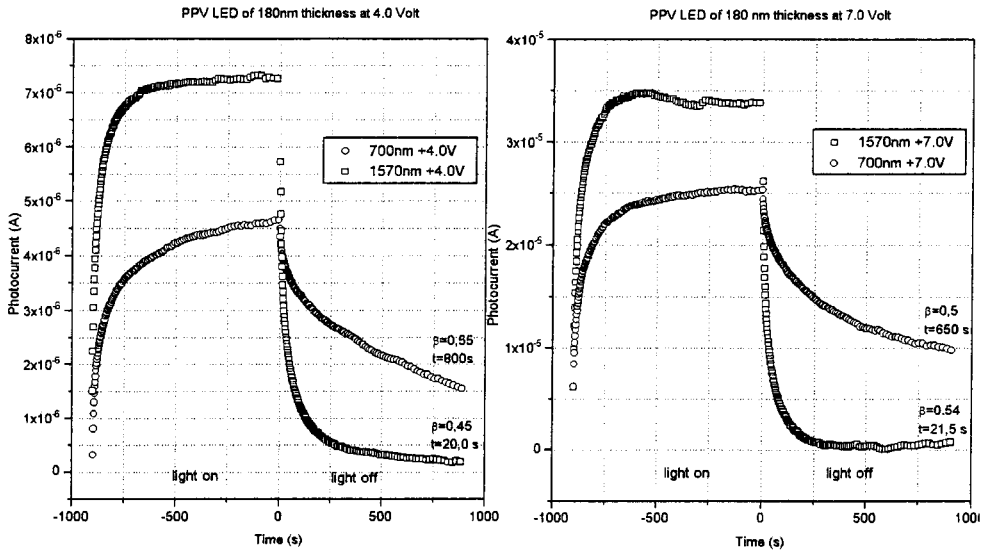

Fig. 4.2 Transient currents at two different voltage and wavelenghts. The rising curves gives the light on situation and the decaying curves the light off. The highest voltage gives a larger photocurrent which scales with the IV curve of the sample..

enough to describe the complete time dependence of the polymer. Because the choppingtime is too small for reaching steady-state this means that the lock-in is measuring on the rising and decaying curve of the photocurrent. Only a small fraction of the total photocurrent will be measured now because the current doesn't has enough time to reach it's maximum value. Figure 4.2 immediately shows that the IR has the fastest response and therefore a lock-in technique measures the highest QY for the IR as is shown in the QY spectrum of figure 4.1. From figure 4.1 we can also see that the QY spectrum is higher for smaller chopping frequencies. At high chopping frequencies we measure almost no photocurrent at all. This states once again that a lock-in technique is not suited for measuring the persistent photoconductivity. Furthermore, it is observed that the QY spectrum is totally independent of the contact used [8]. From this we can conclude that the excitation caused by the light, mainly effects the bulk of the polymer and therefore IPE spectra are not measured.

So, in conclusion the LIA measures the highest QY for the longest time-interval and the fastest response. The difference between two wavelenghts depends on the way the system relaxes to its final value for each wavelenght. Shortly, we can state that the measurement of the QY with a lock in technique *is not representative for the absolute value of the photocurrent but more for the relaxation of the photocurrent.*

§ 4.2 Trapping in hole-only devices.

§ 4.2.1 modelling of the photoconduction experiments.

Because of the slow relaxation, the following transients are now measured with the picoamperemeter and the voltage source. The photocurrent at two given voltages is now obtained by the difference between the steady-state with the light on and the steady-state background current

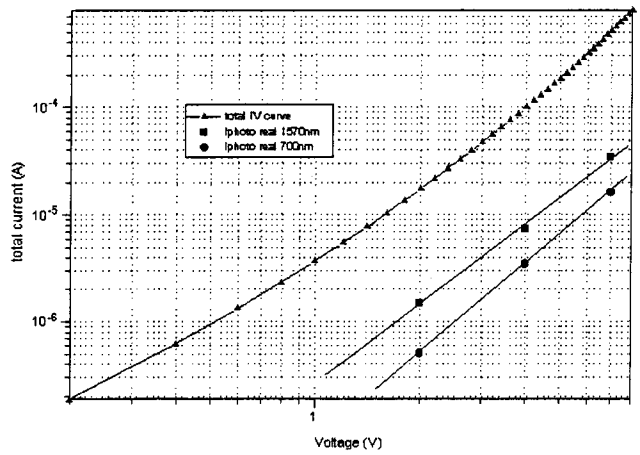

Fig.4.3 Measurement of the photo IV curve without the LIA. The normal IV curve is also shown on a log-log scale.

with the light switched off. The normal IV curve together with the real photo IV curve calculated from the relaxation curves are shown in figure 4.3. Measurements are done with $E_{photon}<E_{gap}$. It is shown that the real photocurrent is larger for higher voltages and is always about 5% of the total current. The total I-V characteristic shows a fully SCL current and therefore the trapping should be small. In general it is found that the real photocurrent scales

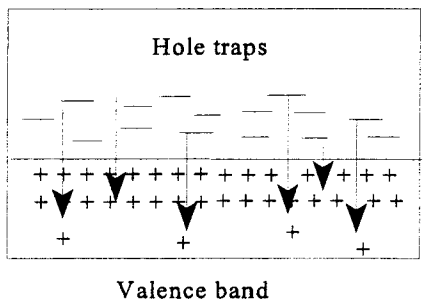

Fig. 4.4 Illustration of the photo effect. The picture shows detrapping of deep traps, increasing the free carrier density in the valence band..

with the total IV curve and that the relaxation process is indeed only a small fraction of the total current (5%). This indicates that the current can be slightly increased with the light due to carriers which are released from the traps. This is schematically shown by figure 4.4. Slow relaxation of the current is then expected to occur for deep traps which have a long escape time (see also equation 2.13).

Slow transient currents shown by figure 4.2 are reminiscent of the persistent photoconductivity in organic and inorganic semiconductor systems[24]. As shown by figure 4.5 the observed relaxation is not a normal exponential (Gaussian) relaxation. Lee et al[15] already found this slow relaxation in PPV for light excitations above the bandgap. They found this relaxa

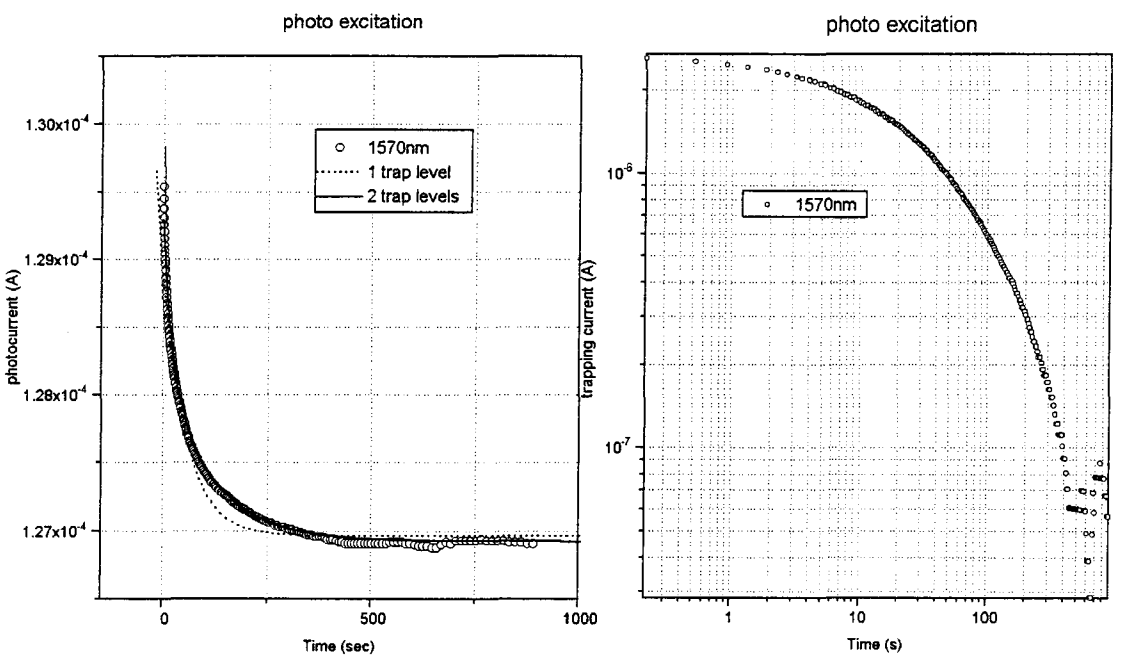

Fig.4.5 Typical slow relaxation of the current due to photoexcitation. An one exponential fit is not enough. Two traplevels is already enough to fit the curve. The right figure shows the same photo transient on a log-log scale. As can be seen the relaxation does not show a power law time dependence.

tion in a surface-cell configuration where gold electrodes were evaporated onto the top surface of the polymer film. From the theory one should expect a power law time dependence but this is not observed as can be seen in the right figure of 4.5. It seems that the relaxation exhibit another non-exponential relaxation.

A possible explanation for this non-exponential relaxation is time dependent diffussion which leads to a commonly used law for relaxation. This well-known relaxation law is widely used now for explaining relaxation processes in a wide variety of random systems and is given by:

$$I(t) = I_0 e^{\left(-(\frac{t}{\tau})^{\beta}\right)} \qquad (4.2)$$

Here I(t) is the current. Several mechanisms leading to this type of relaxation have been proposed [18,19,20,21,22]. However, the underlying mechanism for this so called "strechted exponential" relaxation comes originally from the diffusion of particles in a medium[14] (in the original Debye model these are fluid particles randomly hitting molecules).

Although the physical processes which generate this strechted exponential are still controversial, two classes of models have been proposed. One postulates a statistical distribution of lifetimes of many uncorrelated degrees of freedom (parallel relaxation). In this case the functional form follows from the probability distribution $\psi(t)$ [14]. The other model proposed a serial relaxation to equilibrium via a hierarchy of dynamical constraints. The latter model offers us a greater physical insight into the mechanism than the first model. It postulates a time dependent relaxation rate k(t) so that the relaxation processes are no longer independent of each other. The decay of the excited carriers can be formulated with the following rate equation[15,23]:

$$\frac{\partial n(x,t)}{\partial t} = -k(t)\,n(x,t) \qquad (4.3)$$

Recently, the strechted exponential has been explained via a power law time decay or diffussion in hydrogenated amorphous silicon [23]. The dispersive diffusion is explained due to the motion of bonded hydrogen. By substituting a power law time dependence for the rate constant like $k(t) \sim t^{-(1-\beta)}$ in formula 4.3, the stretched exponential can be obtained by integrating this formula. The time dependent rate constant states that when time grows, the rate constant becomes smaller. This means that the diffusion of defects is slower when time progress.

Lee et al[15] also used this strechted exponential to fit the data and gave an explanation based on the above given diffussion mechanism. They proposed that bipolarons, created in the bulk of the polymer film, diffuse to the surface where they dissociate into polarons. These bipolarons give rise to the observed transient because the long lived bipolarons are less mobile than polarons. However, we found the same kind of relaxation in another configuration (there is no surface) for light frequencies below and above the bandgap and also for a step voltage excitation. Also now, the strechted exponential can, indeed, fit our results. The fitting parameters for the photoconductivity experiments are the same as found by Lee et al[15] (These parameters are displayed in fig.4.2). From this we can conclude that we are looking at the same kind of relaxation mechanism. Because we have no surface in our sample, an explanation as given by Lee et al[15] is not consistent with our experiments. In another way, a diffusion mechanism that is related to the slow relaxation in a PLED is not very obvious. The presence of deep traps with long release times are also a good candidate for slow relaxations in a material (see the theory). Therefore, we use a (semiconductor) trapping model as described in the theory.

The semiconductor trapping model.

The model used here, assumes that carriers can be trapped and detrapped from defect states instead of diffusion of the defect states. If we assume that holes are trapped and detrapped from deep trap sites and it is known that the trapping is small in hole-only devices, an estimation for the trap depht and the trapping density can be made. If a voltage is applied, the free carrier concentration is about 10^{22} m^{-3}. Compared to the amount of trapping (5%) in hole-only

devices this indicates that the amount of active traps is something like 10^{20} m^{-3}. If we start with the simple case of one trap level, this level should be deep enough to give slow trapping times. Because the relaxation is on the second time scale a first estimation for this traplevel is about 0.8 eV which can be found from equation 2.13. Trap levels closer to the valence band results in shorter escape times. Most of the traps are, according to the I-V characteristics, already occupied and therefore the Fermi level is close to the valence band. If the Fermi level is about 0.3 eV, most traps are filled and N_t-n_t is small leading to a slow capture time according to equation 2.14. The figure on the right illustrates how the parameters are used in the simulation. The perturbation arises from the light. Because the bulk of the polymer is homogenously excited the traps will be partially emptied by the light. Therefore the total amount of trapped charge at t=0 is somewhat lower due to the light than follows from the thermal equilibrium conditions. This contribution is estimated to be about 5% of the free carrier concentration.

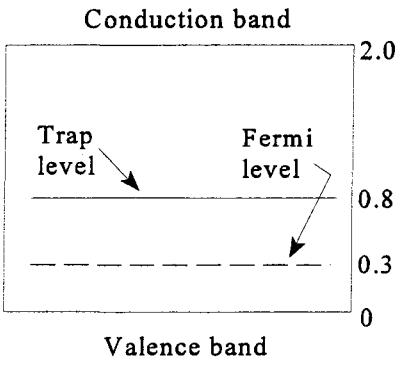

Example of how trap level and fermi level are used in the simulations.

Unfortunately, it seems that the band trapping model is, until now, not suited for explaining the transients quantitatively. Taking the trapsites and fermi level as described above results in slow trapping times but then nearly all traps are filled and there is almost no trapping. An effect of 5% can not be reached. Putting the Fermi level around 0.6 eV, more traps are empty resulting in a larger trapping effect but the relaxation shifts to the millisecond or even microsecond timescale. It is not possible to choose values that corresponds to the observed effect of 5% and the right relaxation times. In another way, a relative large trapping effect combined with a relaxation on the experimental timescale is not possible.

The main difficulty in using the semiconductor trapping model is the phonon frequency of equation 2.13 (~10^{12} Hz) that determines the escape time which is used for further calculations. It has been found that if the escape time is small, the relaxation is always too fast. Lowering the phononfrequency is the only alternative to reach a slower response and then it becomes possible to fit the experimental observations with the trapping model. In figure 4.5 it is shown that the photocurrent can very well be fit with the trapping band model if at least two trap levels are used. For these fits an arbitrary value of one is used for the phonon frequency. Because the escape time is used for the calculation of the other equilibrium values, the dynamics of the trapping is not influenced by changing the phonon frequency. Although the whole curve is shifted from the microsecond time scale to the second timescale, the trapping model still reveals the same relaxation curves. In this view we can accept the model if we make only qualitative conclusions.

Apparently, another contribution should be added to the model to be able to fit the experiments quantitatively. In the hole-only devices the current is fully SCL and therefore the current relaxation might be altered because of the non constant electric field. In the proposed model, these space charge effects are not yet taken into account and the electric field is taken to be constant. However, Many et al[16] found an approximate exponential solution for the trapping problem in a SCL system. This solution has been found for one trap level with a very low occupation. From this it is clear that space charge effects probably have a small influence

on the relaxation in polymer LEDs. However, a band of traps is expected with a high occupation and this may change the solution found by Many et al[16]. Implementation of the trapping model into the SCL model is one of the things that will be done in the future.

Instead of using a pure semiconductor band model where the carriers can freely move in the valence band, it is also possible to introduce hopping conductivity. Hopping transport in a polymer is probably more realistic to think of due to the disorder. In a hopping system there is no band where the carriers can freely move but exist of localized states. If the overlap between the wavefunction of the sites is large enough conduction can take place. For higher energies this carrier transfer step is more probable. This idea is described in 2.8.1 where a power law time dependence has been found. However, plotting the current-time characteristic on a log-log scale (inset of figure 4.5) doesn't show a power-law time dependence. Nevertheless, formula 2.19 is the same as used for the semiconductor model except for the prefactor in the hopping rate: $\nu_0 \exp(-2R_{if}/a)$. This factor is introduced due to the extra barrier which exist in the case of hopping because hopping not only occurs to higher energy but also to other distances. In a semiconductor this factor is not relevant. Therefore, in the hopping case it is possible to have a large escape time while the traps can still be close to the valence band which is for a pure semiconductor not possible. The difference between hopping and trapping in a semiconductor is shown in figure 4.6. Unfortunately, it is not known how large this value

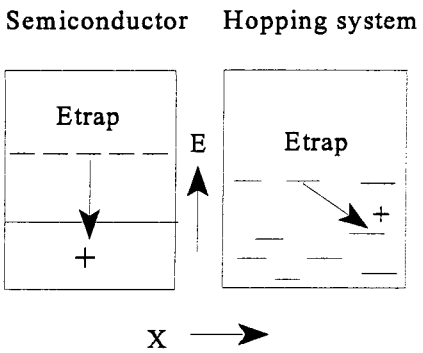

Fig.4.6 Difference between trapping in semiconductors and in a hopping system.

is but it is not unlikely that this factor reduces the prefactor several orders of magnitude. In that case a quantitative description might be possible. Hence, the introduction of hopping reduces the prefactor in the semiconductor model and therefore it is possible to make a quantitative fit to the experiments.

§ 4.2.2 Qualitative explanation of the transients.

With a phononfrequency of one it has been shown that it is possible to make a good fit although it is not necessary to take this low value. The only reason is that calculations are easily performed with this value. To get a better understanding of what happens during the trapping process and why the long tail in the relaxation appears due to trapping, simulations have been done to illustrate this (with $\nu_{phonon}=1$). For simplicity the calculations are done for electron trapping but a similar analysis can be carried out for the holes. A schematic presentation for the simulations is given in figure 4.7 and the resulting simulations are shown in figure

4.8. The curves are calculated for three different Fermi levels and two constant traplevels with the same N_t. In the case that we have the Fermi level below the two trap levels (case 1) we see the long tail appear in the curve. The relaxation is faster and the long tail disappears when the Fermi level is lifted and the rela tive trapping effect becomes smaller. If the Fermi level is below the trap sites, the traps are almost completely empty. Because the deepest traps have the longest escape and capture time it takes longer before this trap level is in equilibrium. The occupation of the deep traps are larger because they are closer to the Fermi level and so the capture time of these traps are also larger. Therefore, in the case that the deep traps are completely empty, the capture and release of these traps are responsible for the slow, long tail relaxation. If the Fermi level is between the two trap levels, (case 2) the deep traps are in thermal equilibrium already mostly filled and therefore the long tail dissapears. For the Fermi level above the trap sites (case 3) we have all traps almost completely occupied in thermal equilibrium resulting in a small trapping effect. The deep traps are certainly occupied now and will not participate in the

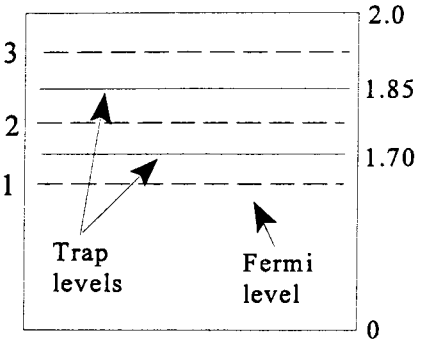

Fig.4.7 Schematic illustration of the position of the trap levels and the Fermi level for the simulation of figure 4.8.

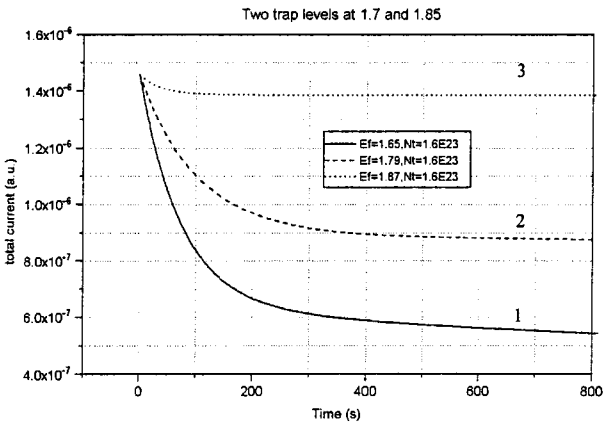

Fig.4.8 Illustration of the existence of the long tail in the transient curves and the influence of occupied trap levels on the relaxation..

relaxation anymore. Only a few fast trap sites can be occupied with free carriers now and the relaxation will be fast and small. With these simulations it is also shown that the transients can qualitatively be very well understood with trapping dynamics.

§ 4.2.3 Spectral photoconduction.

As is clear from §4.2.1, the required dispersion to fit the experiments is too small when one trap level is used. A plausible extension to introduce dispersion is a multiple trapping regime (as mentioned in the theory). This multiple trapping regime can exist of some discrete levels at different energies (shallow and deep traps) each with a different characteristic time constant. For the photoconduction experiments it was found that two trap levels already introdu-

ced enough dispersion to fit the curves. For a disordered system as PPV it is more realistic to think of a distribution of trap level energies. Summation of the relaxation curves gives the dispersion. Matsuura et al [25] also related discrete trapping levels with the current relaxation in silicon nitride (SiN_x). They were able to determine the trapping density with two discrete levels. For each level an exponential curve without the effects of trapfilling was used. However, the occupation of traps is in hole-only devices significant.

The photoconduction experiments are fit with a multiple trapping regime (with $\nu_{phonon}=1$) with an exponential distribution of the traps. The light excites the polymer which can be introduced as an increase in the free carrier concentration and deternines the absolute trapping effect. The multiple trapping regime exists of 10 levels spaced 0.02 eV from each other. For the fitting parameters the exponential DOS given by formula 2.6 is used. The fitting parameters used are schematically shown in figure 4.9 where dp_0 is the free carrier concentration generated by the light. Furthermore the Fermi level is introduced which determines the

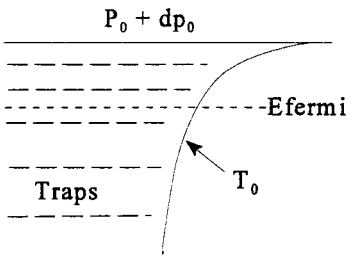

Fig.4.9 Different parameters as used in the simulation. The traps exhibit an exponential distribution.

relaxation time and T_0 gives the typical width of the trapping regime and determines the exponential distribution. By exciting the polymer with the light, one expect that the all parameters have the same value for different wavelenghts except for the amount of excitation dp_0. It is found that this photo excitation scales with the light intensity of the lamp if the other

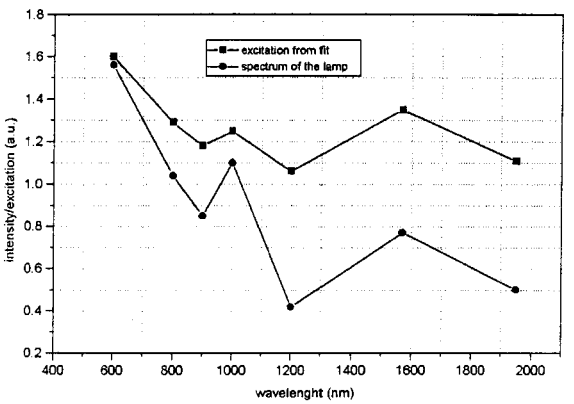

Fig. 4.10 Excitaton found from the simulation for different wavelenghts compared to the spectrum of the Hg lamp. The excitation parameter follows almost excactly the spectrum of the lamp.

parameters are kept constant as shown by figure 4.10. With this DOS we were able to fit the experiments if we take $T_0 = 700K$. A larger value for T_0 gives a bad fit for the transient at small times. Evidence for taking this exponential DOS comes from the IV-characteristics and formula 2.7. Because the fit can only be interpreted as a qualitative result, it is very difficult to give an explanation for the difference in scaling constant. Nevertheless, from figure 4.10 it seems that the trapping is nearly independent of the exciting wavelenght.

§ 4.2.4 Voltage step relaxation.

Besides excitation of the hole-only device with light it is also possible to excite the polymer by turning on and off the voltage. Figure 4.11 shows a typical example of the transient observed from a voltage step excitation. It can be seen that the relaxation is even slower than the transients resulting from the light pulse. Just as was found from the photoconduction experiments, the transient of the voltage step doesn't show a power law time dependence as

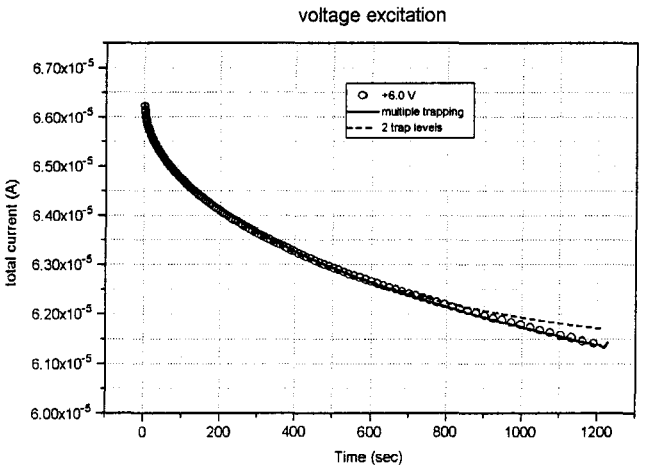

Fig.4.11 Typical transient resulting from a voltage step. Two trap levels are not enough to fit the whole time domain. A multiple trapping regime gives a good fit.

should be expected from the theory. Because the excitation is given at the electrode, the charge distribution in the polymer is not homogenous as was the case for the light excitation. Therefore a gradient in the conduction current is introduced. Because the injection of the charge carriers from the electrode into the polymer doesn't release carrier from traps, the begin condition for the occupied traps is not changed. This is in contrast to the light case where the begin conditions were altered due to release of charge from traps. Despite of the difference in begin conditions, the same problems with the semiconductor trapping model as described for the light excitation occured. Also now the phonon frequency is the only way to obtain a slow relaxation. Taking this value one as was done for the photoconduction experiments makes it possible to fit the curves very well. The slower relaxation indicates that the introduced dispersion due to the traps is larger now. Fitting the curves with two trap levels showed that the introduced dispersion is not enough to fit the whole transient. For large times the fit deviates from the experiment. Therefore the introduction of an extra (deep) traplevel is required to be able to fit the whole transient. This ones again indicates that a multiple trapping

regime is more appropriate for the hole-trapping. Using the multiple trapping regime as found from the photoconduction experiment shows that with this trap distribution the curves can be fit. For the typical width of the traps it was necessary to take a value of T_0=700K otherwise the curve doesn't fit the short times for higher values of T_0.

From the photoconduction and voltage step experiment we can conclude that the traps are exponentially distributed with a typical width of T_0=700K. Because the functional form of the relaxation is not changed by taking a lower phononfrequency we are able to make this conclusion because the trap distribution is only determined by the functional form of the transient.

§ 4.2.5 Influence of the conduction current on trapping.

A further refinement to the model can be introduced by using the particle conservation law in his complete form. A different distribution of carriers in the polymer leads to a gradient in the conduction current. Voltage step experiments introduce this gradient in the conduction current because the carriers are injected from the electrodes. To investigate the influence of this gradient on the trapping, some simulations have been done. The polymer is divided in a set of discrete distances. On every distance x we can add one or more trap levels. For simplicity we assume that for every trap energy, N_t is the same on every distance. In real polymer LEDs this may not be true due to the disorder. If the excitation is homogenous over the distance (this is in the case of illumination) all the free carriers will be trapped for every distance in the same way. Therefore, the gradient dJ_c/dx will be zero at every time t. In this case we have the simple model with $dJ_c/dx=0$. If we put the excitation at t=0 only on the interface (this is the case for the voltage step) of the polymer LED (delta function excitation), a gradient dJ_c/dx will be introduced immediately after this excitation. Free carriers at a distance x will not only be trapped at that distance but will also be distributed over the polymer according to the introduced gradient. Due to this change of the conduction current in the x direction, the number of free carriers is not homogenous at different distances. Therefore the relaxation due to trapping may be different now. To obtain the total current one integrates over the sample thickness:

$$I(t) = \frac{1}{L}\int_0^L J_c(x,t)dx = \frac{1}{L}\int_0^L q\mu n(x,t)E(x,t)dx \qquad (4.4)$$

We see that I(t) is the space average of the conduction current. For simplicity we ignore space charge effects and assume E(x,t)=V/L=constant. Simulations with this gradient in the conduction current are shown in figure 4.12. From the left figure we see that the conduction current becomes stable on a millisec. time scale. Because the experiments show a relaxation on a time scale of several minutes, the conduction current has no influence at all on the relaxation. By taking the phonon frequency several orders of magnitude larger we can "manually shift" the trapping process to the millisec. time scale. This is shown in the right figure. The change in the conduction current is not influenced at all by this time shift of the trapping process. From this we can conclude that the change in conduction current always works on the millisec. timescale and therefore has no effect on our experiments. From the right figure we also see that trapping is only a small fraction compared to the change in the conduction current. The

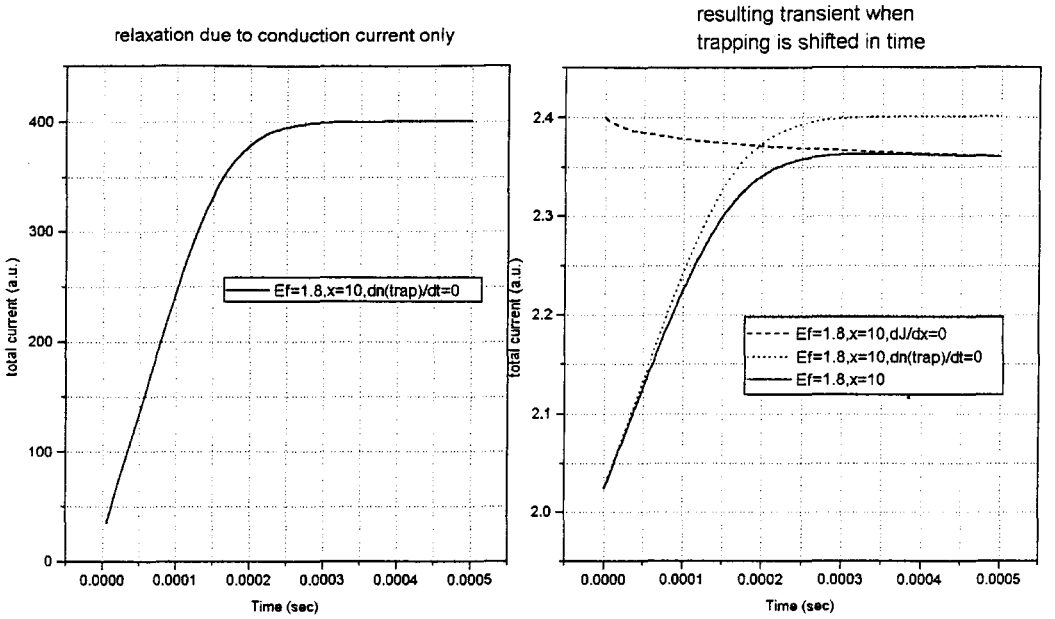

Fig.4.12 Influence of a gradient in the conduction current on the total relaxation. For the simulation L=0.3 um and V=4.0 was used.The left figure illustrates that the conduction current reaches it's final value within a few millisec. The right figure shows that the conduction current is still the same if we shift the trapping process to millisec. scale.

trapping effect is about 10% of the stable current, a number we also found from the experi ments. Furthermore, a transit time, defined as the average time carriers need to reach the other electrode, can be read from the right figure. Because the current becomes stable around $2.5*10^{-4}$s, most of the carriers have reached the other electrode and so this is equal to the transit time. This transit time is in very good agreement with the value obtained from formula 4.1. In conclusion we can say that if the system is inhomogenously excited, we have a quasi steady-state situation if we measure at times much larger than the transit time. Therefore, on this experimental timescale the differential dJ_c/dx can be ignored.

§ 4.2.5 Temperature dependence of a hole-only device.

To investigate the multiple trapping model further we can make use of the temperature. From the above we know that we need a multiple trapping regime to be able to fit all the experi- ments. Because we are using a semiconductor model, the familiar semiconductor statistics can be applied to the temperature dependence of the p-doped hole-only LED. From Sze[4] it is found that when temperature decreases, the Fermi level in a p-type semiconductor as our polymer will come closer to the conduction- or valence band according to the formula:

$$E_F - E_v = k_b T \ln\left(\frac{N_v}{N_A}\right) \tag{4.5}$$

For small acceptor densities, as in our PPV, the shift of the Fermi level as function of the temperature is larger than for high doping densities.

The temperature dependence is investigated with a voltage step experiment. The sample is

biased at 12.0 Volts in order to measure enough current at low temperatures to get a reliable transient. In practice we find that the transient curves are very sensitive to small changes in the temperature making them useless for changes larger than 0.1-0.2 K. For these temperature changes, the deviation of the background current is larger than the total trapping effect. The temperature is controlled by a liquid nitrogen flow along the sample. Keeping the temperature stable within 0.1 K was only possible for short measuring times.

The left figure of figure 4.13 shows the relative trapping effect for four transients at different temperatures. The right figure shows the experimental fit with the multiple trapping

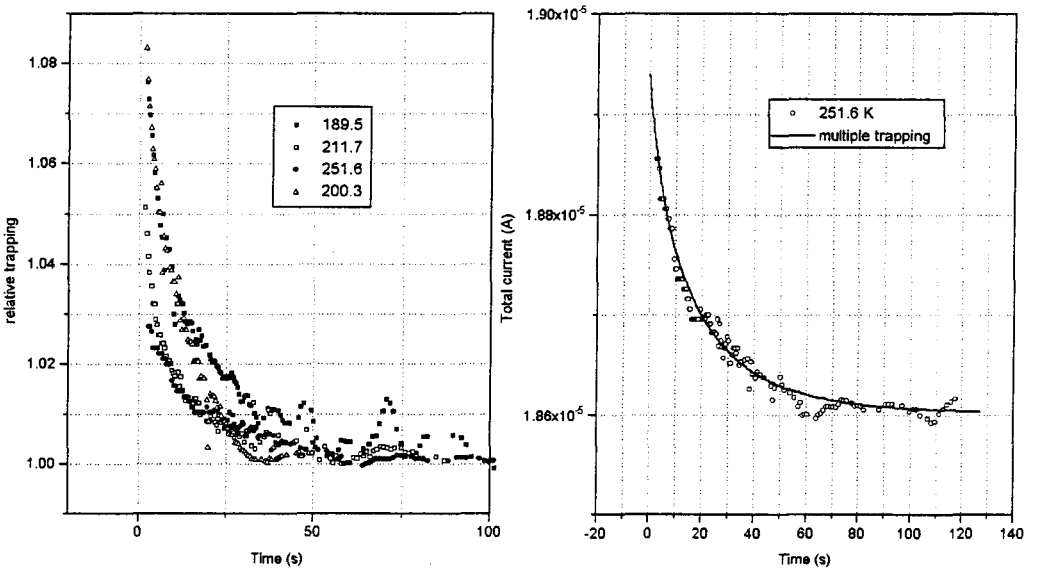

Fig. 4.13 The left figure shows the relative effect of the temperature on the trapping. As can be seen, the time before steady-state is reached is reduced. The relative trapping effect is always of the same order. The right figure shows the experimental fit with a multiple trapping model for 251 K.

model using an exponential DOS as found from the voltage step and the photoconduction experiments. The left figure illustrates that, within the accuracy of the measurement, the relative trapping effect is the same for different temperatures. Because the current decreases with temperature, a similar result as given in figure 4.3 is obtained. This ones again indicates that the trapping scales with the current.

Furthermore, from the voltage step experiments we know that the relaxation at room temperature is much slower. The time it takes to reach steady-state is for low temperatures two orders of magnitude smaller. The faster relaxation can immediately be understood with figure 4.8 and the fact that the Fermi level is closer to the valence band for lower temperatures resulting in a faster response.

In short, the temperature measurements shows that the relative trapping effect is independent of the current and that the relaxation becomes faster for lower temperatures.

§ 4.3 Trapping in electron-only devices.

§ 4.3.1 The current-voltage characteristic.

The relaxation of the current in electron-only devices was also a subject of this study. Because gold has a high work function, it is almost impossible to inject electrons from the gold electrode into the polymer. To get a low barrier for electron injection in the polymer LED, we need metals with low work functions. Calcium is a suited contact material for this purpose. The disadvantage of materials with low work functions is the fast oxidation in air. Because of this the transient voltage step experiments are done in a nitrogen atmosphere. Photoconduction experiments were not possible in this nitrogen box.

From current-voltage measurements we found that the current in these devices is very small compared to the hole-only samples. Furthermore, the current in electron-only devices is not fully space charge limited as we found for the hole-only devices but has an ohmical region with very small currents. Figure 4.14 shows the IV curve of an electron-only sample.

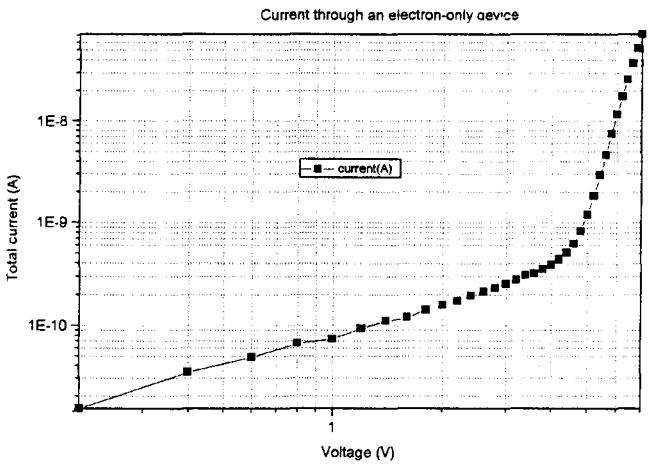

Fig.4.14 Current voltage characteristic of an electron-only sample on log-scales. The first part of the curve shows an ohmical behavior. The slope of this curve is 1.07.

From this figure we immediately see the difference with a hole-only sample. Relatively high voltages are needed to get only a small current (in the order of nA) through the sample. For thicker sample we even need about 30 Volts to obtain the same low current. In contrast to the hole-only samples a sharp transition from an ohmical region to a region with $J \sim V^n$ ($n \sim 8$) is observed indicating large trapping. From the slope of this curve we can, according to formula 2.7 determine the typical width of the trapping regime. From this formula we obtain T_0=2000K. So far, it was not possible to measure higher voltages because these voltages destroys the sample. The voltage where all the traps are filled and the current is fully space charge limited can therefore not be observed.

§ 4.3.2 Current relaxation in electron-only devices.

Transient curves can be measured on these samples only in the low current regime otherwise

the sample will be destroyed. To be able to measure these curves, the highest voltage possible is taken. For the sample of figure 4.14, 7.0 Volts was a reasonable value. We started to measure this sample at 5.0 Volts because the current was high enough to measure the transient at this voltage. The result of this measurement is plotted in figure 4.15 on a log-log scale (where the same sample is used as for figure 4.14).

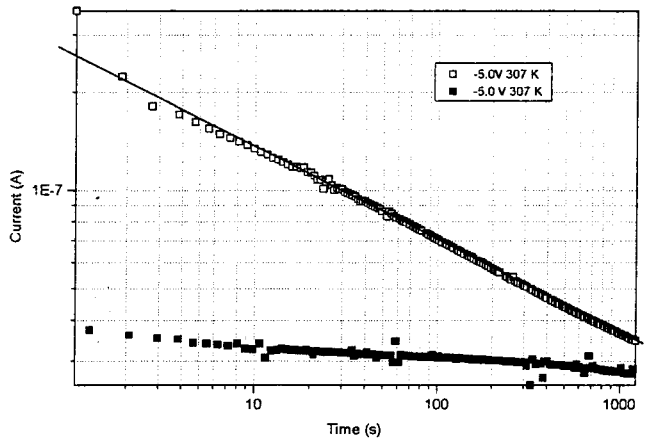

Fig.4.15 Transient of an electron-only sample on a log-log scale when it is used for the first time. The closed squares gives the transient when the measurement is repeated shortly after the first measurement.

From figure 4.15 it appears that the trapping effects are very large for electrons, in agreement with the steady-state current voltage characteristic. The influence of the electrical history is showed in figure 4.15 by the solid squares. This curve is measured shortly after the first measurement (open squares) was done. As can be seen the trapping starts at the point where the first experiment ends. This can qualatitively be explained with a multiple trapping model. The first time the traps are completely unoccupied. The trapping effect is therefore very large. As time progress deeper traps also become occupied resulting in the slow relaxation. When the voltage is turned off and shortly after it a new transient is measured, it seems that all the traps which were occupied in the former experiment are still occupied. This is because the sample is still charged. By switching on the voltage, the voltage source does not have to supply additional carriers to the sample. Therefore, the electrical history of the sample determines completely the transient in this case. Apparently, the escape time from these traps is very large.

As expected from the current voltage characteristics there is, compared to the hole-only samples, a dramatic difference in the amount of trapping. The electron current almost completely disappears (over about one order of magnitude) when time progress in contrast to the hole-only samples where the trapping is about 5% of the steady-state (background) current. Furthermore, the electrical history doesn't has a large influence on the hole-only samples as for the electron-only samples because most of the traps are already empty before the next experiment starts. This indicates that the average escape times are smaller for hole-only samples than for the electron-only samples. A possible explanation for the large differences in trapping behavior of electrons and holes might arise from the fact that PPV is p-type semiconductor. Then the Fermi level is located relatively close to the valence band, which means that

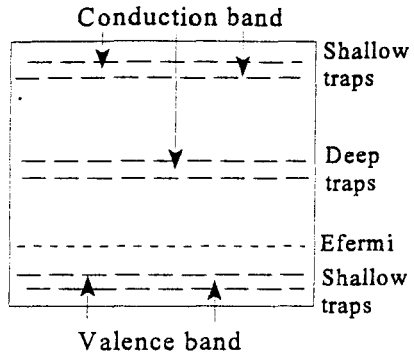

Fig.4.16 Possibilities for electron and hole trapping.

the deep (slow) trap levels around midgap are unoccupied, as schematically indicated in figure 4.16. These unoccupied levels are able to trap electrons but do not trap holes.

From this we can conclude that the current-voltage characteristic not only changes due to the history of the sample but that the time before the current is readout also plays an important role. Therefore it is important to realise wether the current is read out after 1 seconds or after 1 hour. Because the current decreases in time, the measured current will have a different value at different times. Figure 4.14 is measured in a few seconds and therefore gives a current that is too high compared to the steady-state value of the current. Figure 4.17 gives two IV charac-

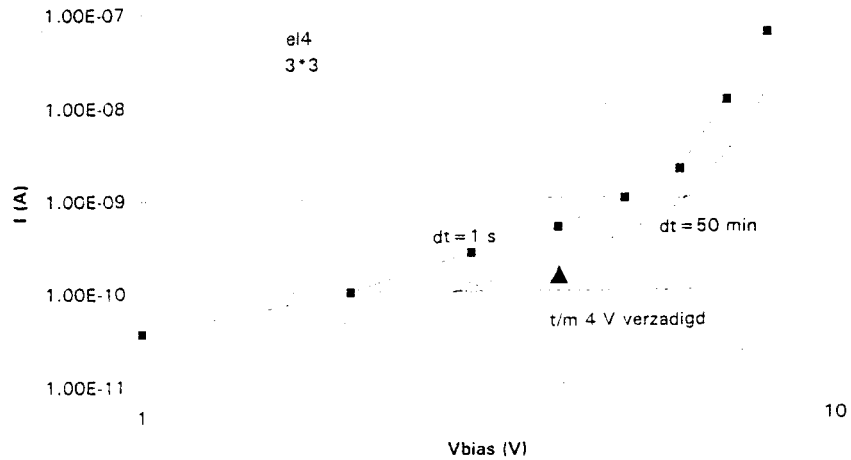

Fig.4.17 Difference between two IV characteristics when the time between switching on the voltage and the current readout is varied.

teristics where the time between switching on the voltage and the readout of the current is varied. The highest current results from the shortest waiting time which is expected. Furthermore, it seems that the transition to the SCLC is not so abrupt for the long waiting time (dt=50 min.).

Another difference with the hole-only samples is that the trapping current follows a power law time dependence as should be expected from the random walk theory. On a log-log-scale this gives a straight line as shown by figure 4.15. This is not the case for the hole-only sam-

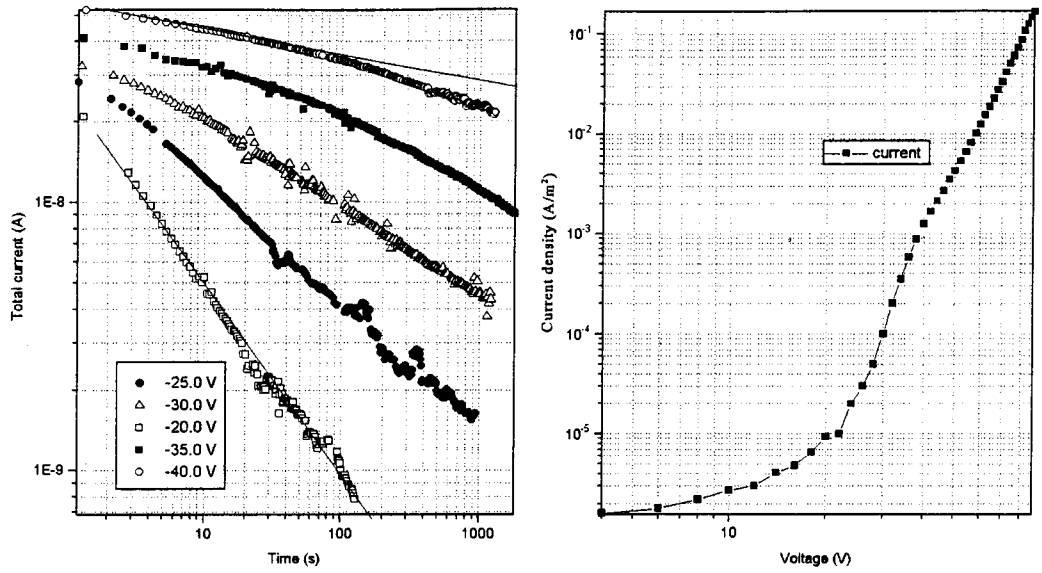

Fig.4.18 Transient curves at different voltages for an electron-only sample on a log-log scale. The left figure shows straight lines until -35.0 Volt. Furthermore we see that the slope is smaller for higher voltages indicating the occupation of traps due to the earlier experiments. The right figure shows theJ-V characteristic from the left figure. Deviation from the straight line appears when there is an abrupt increase in the current.

ples. Figure 4.18 shows some transients at different voltages. Just like figure 4.15 we see the power law time dependence. From the left figure we see that a deviation from the straight line appears for voltages above -30Volt leading to curves similar to those of the hole-only samples. From the IV curve (shown in the right figure) it follows that the kneepoint is around this voltage. Apparently, the ohmical region results in a power law time dependence and the space charge limited region to curves described by a trapping model. Furthermore, the trapping effect becomes smaller for higher voltages as is expected, since for higher voltages the filling of traps increases.

It is not possible to fit these experiments with the multiple trapping model as used for the hole-only samples. Nevertheless, we can explain these curves very well with the more dedicated random walk theory in an exponential multiple trapping regime as described in 2.8.1. For the electrons the observed current relaxation follows the expected $I(t) \sim t^{-(1+\alpha)}$ until the trap filled regime is reached. When the traps are filled the measurements starts to deviate from the power law time dependence and is not in agreement anymore with the random walk theory. It should be noted that for the holes also most of the traps are filled and that the relaxation also deviates from the random walk theory. Thus the question arises whether the random walk theory is still valid when most of the traps are filled.

§ 4.3.3 Temperature dependence of the electron-only LED.

From the predictions of hopping transport in a multiple trapping regime there should be a temperature dependence in the relaxation. From the slope of the curves at different temperatures, a typical width T_0 for the multiple trapping regime could be determined. This value can be

compared with the value found from the IV characteristic. To avoid history effects, we measured one transients per day so that the sample has enough time to "recover". The results of these temperatures measurements are shown in figure 4.19. It was not possible to make the

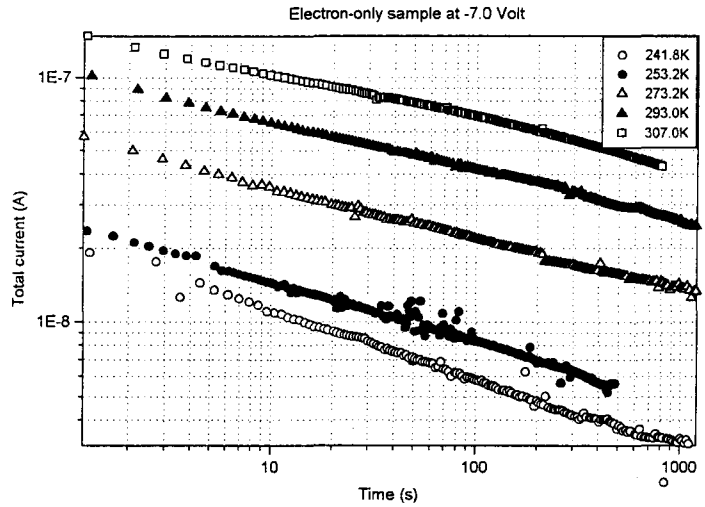

Fig.4.19 Transient curves at different temperatures. As expected from the hopping theory, all the curves gives straight lines on a log-log scale. Although the variation is small, the slope for lower temperatures is larger.

temperature lower than 240K because the current became to small to be measured. It follows from the figure that the slope for lower temperatures is larger than for higher temperatures although the variation is small. This indicates that the typical width T_0 of the multiple trapping regime is relatively large resulting in a small variation of the slope in the measured temperature range. However, this variation in the slope is qualatitively in agreement with the hopping theory. A more quantitative evidence for the theory is given by figure 4.20. If we fit the curve with a power law like $t^{-\alpha}$ we can determine the typical width T_0 from this slope. Putting $(1-\alpha)$

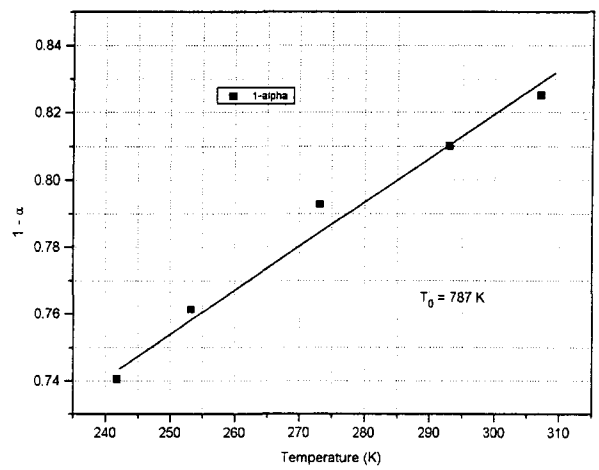

Fig. 4.20 Determination of the typical width of the multiple trapping regime from the temperature dependence of the transient curves. From this line we find T_0 = 780K.

against the temperature gives a straight line with a slope proportional to the reciprocal of T_0 according to the power law time dependence. This is done in figure 4.20. As can be seen this curve is perfectly in agreement with the theory and the typical width of the trapping regime determined from this curve is approximately 750K. The value found from this hopping model is smaller than the value found from the IV characteristics. However as figure 4.17 shows, the typical width is smaller if the IV curve is measured in a more steady state situation. This can qualitatively explain the difference between the two values. The value found from the IV characteristic gives an over esimation for T_0. The typical width found from figure 4.20 also reminds us to the value found from our multiple trapping regime for the hole-only samples. For those fits we had to take a value for T_0 of approximately 700K to be able to fit the whole curve. In the hopping theory, the same exponential DOS is assumed.

From these experiments we can conclude that the multiple trapping regimes for the holes and for the electrons are the same. Furthermore deviations from the random walk theory seems to occur when the traps are filled.

5. Conclusions.

Current transient measurements have confirmed the results of steady-state current voltage experiments: the trapping in hole-only devices is very small whereas the trapping in electron-only devices is very large. The current transients have been described usinf a multiple trapping model. Quantitatively, the reultst of this multiple trapping model are not in agreement with the observed transients. However, by reducing the escape and capture rates, the strongly non-exponential current transients are well described by the multiple trapping model using an exponential distribution of traps with a typical width of 700K. A better quantitative agreement might be obtained by including hopping into the escape and capture rates. Spectral photoconductivity reveals that the current relaxation in hole-only devices is nearly independent of the exciting wavelenght.

Current relaxation in electron-only devices are in agreement with the predictions of a more dedicated random walk theory. It is found that the width of the trap distribution T_0 is approximately the same as found for the hole-only devices. Furthermore, it appears that the experiments deviates from the predictions of the random walk theory when the traps are filled, resulting in transients similar to those found for the hole-only devices. Finally, it is demonstrated that the electrical history of the electron-only devices plays a vital role in the determination of the IV-characteristics.

Bibliography

[1] M. Pollak, B Shklovskii: Hopping transport in solids, by S. Roth, North Holland , Amsterdam (1991).
[2] C. Kittel: Introduction to solid state physics, sixth edition, J.Wiley&Sons, New York (1986).
[3] A. Heeger: Rev. Phys. Mod. Vol.60,No3, july 1988.
[4] S. Sze: Physics of semiconductor devices, second edition, J.Wiley&Sons, New York (1981).
[5] I.D. Parker: J. Appl. Phys. 75 (1994) 1656.
[6] J. Levinson: Mol. cryst. Liq. cryst. 26 (1974) 329.
[7] R. Fowler,L. Nordheim: Proc. Roy. Soc. London A 119,173 (1928).
[8] M. Meeuwissen: Photoconductive properties of poly LED devices, Philips Resesarch 1996
[9] A. Patsis,D. Seanor: Photoconductivity in polymers; an interdisciplinary approach. Technomic publishing Co., Westport, 1976.
[10] J. Mort,D. Pai: Photoconductivity and related phenomena, Elsevier scientific publishing company, Amsterdam. 1976.
[11] EG&G Brookdeal electronics: Operating and service manual, Princeton 1986.
[12] P. Blom, M. de Jong: Appl. Phys. Lett. 68 (23) 1996.
[13] Williardson, Beer: Semiconductors and semimetals, Vol. 6 Injection phenomena.
[14] H. Scher, M. Shlesinger: Phys. Today, 26, jan. 1991.
[15] Lee, Yu, Heeger: Phys. Rev. B47, 23,15543.
[16] A. Many, Rakavy: Phys. Rev. vol. 126, 6, 1980 (1962).
[17] Noolandi: Phys. Rev. B16,10,4460 (1977).
[18] Queisser, Theodorou: Phys. Rev. B33, 6, 4027, (1986).
[19] Palmer, Stein, Abrahams: Phys. Rev. Lett. 53, 10, 958 (1984).
[20] Klafter, Shlesinger: Proc. Natl. Acad. Sci. 83, 848, (1986).
[21] Queisser: Phys. Rev. Lett. 54, 3, 234, (1985).
[22] Jiang, Lin: Phys. Rev. Lett. 64, 21, 2547, (1990).
[23] Kakalios, Street, Jackson: Phys. Rev. Lett. 59, 1037, (1987).
[24] general references on PPC i.e. H. Queisser: Proc. of the 17th. Int. Conf. on the physics of semiconductors, San Francisco, (1984).
[25] Matsuura, Yoshimoto: Jpn. J. Appl. Phys. 34 (1995) 185.
[26] S.Heun: J. Phys: Condens. Matter 5,247-260 (1993).

Appendix A.

This is the program which is written to do some simulations on the proposed model. The effects of a conduction current is not included in this program. This program gives the simple case of one distance but offers the possibilty to alter the amount of trapping levels and the density of states for the traplevels. Other parameters can also be changed. The program gives as output, the free carrier concentration as function of the time which is proportional to the current. The simulation program is written for electron trapping but can also be applied for hole trapping.

```
program traps;
{N+}
uses printer,crt;

const  q=1.60218E-19;
       m0=9.1095E-31;
       h=6.62617E-34;
       pi=3.1415927;
       kb=1.38E-23;
       c=1;
       nstep=700;
       scaling=1E26;

type   arraytrap=array[1..c] of real;
       arrayvec=array[0..nstep] of real;
       lijst=record
            tesc  : real;
            tcap  : real;
            pt0   : real;
            cross : real;
           end;
        beginarray=array[1..c] of lijst;

var  m                 : integer;
     Ef,Te,T0,Et,Ntrap : real;
     vphonon,pvrij0    : real;
     p,tijd,pt         : arrayvec;
     Nt                : arraytrap;
     f2                : text;
     start             : beginarray;

procedure evenwicht(VAR k:beginarray;VAR p0:real; VAR Nt:arraytrap);
 var
   Nc,N   : real;
   i      : integer;
 const
   Ec=2.0;

 Begin
   Nc:=2*(((2*pi*m0*kb*Te)/(h*h))*sqrt((2*pi*m0*kb*Te)/(h*h)));
   p0:=Nc*exp(-(Ec-Ef)*q/(kb*Te));                    {p0 is constant for all levels}
   for i:=1 to c do                                   {number of trapdephts}
    begin
     Et:=2.0-(0.05*i);                                {trapenergie}
     Nt[i]:=Ntrap*exp(-((2.0-Et)*q)/(kb*T0));
{      Nt[i]:=Ntrap;                                  {homogeen}
     k[i].tesc:=1/(vphonon*exp(-(Ec-Et)*q/(kb*Te)));
     N:=Nc*exp(-(Ec-Et)*q/(kb*Te));
```

```
      k[i].pt0:=Nt[i]/(1+N/p0);                    {in stationaire toestand}
      k[i].tcap:=k[i].tesc*p0/k[i].pt0;            {evenwichtsconditie}
      k[i].cross:=1/(k[i].tcap*(Nt[i]-k[i].pt0));
      writeln('pt0= ',k[i].pt0);
      writeln('tcap=',k[i].tcap);
    end;
  end;

procedure dndt(p0:real; VAR ka:beginarray; Nt:arraytrap);
 var i,j      : integer;
    dt        : real;
    p1        : real;
    pt1,p2    : array [1..c] of real;

Begin
 dt:=0.005;
 for j:=1 to c do
  begin
   pt1[j]:=ka[j].pt0;
  end;
   p[0]:=5*p0;                          {excitation at t=0}
   tijd[0]:=0;
   for i:=1 to nstep do
     begin
      p1:=p[(i-1)];                     {charge at t=i for all traplevels together}
      p[i]:=0;
       for j:=1 to c do
         begin
           p2[j]:=p1+(pt1[j]/ka[j].tesc-p1*ka[j].cross*(Nt[j]-pt1[j]))*i*dt;      {diff. Equation}
           p[i]:=p[i]+(p2[j]-p1);          {lost free carriers (trapped)}
           pt1[j]:=pt1[j]-(p2[j]-p1);      {increase of trapcharge for every traplevel}
         end;
       p[i]:=p1+p[i];
       tijd[i]:=(i*dt)+tijd[i-1];
       writeln(f2,{tijd[i],}p[i]/scaling);
     end;
     writeln('eindpt0= ',pt1[j]);
     writeln('eind termen=',pt1[j]/ka[j].tesc);
end;

{mainprogram; calculations are in eV, only the number in eV should be given}
Begin
 clrscr;
 assign(f2,'c:\leon\output1.dat');
 rewrite(f2);
 T0:=700;              {These are the start values, T0=typical width of trapregime}
 Te:=308;              {temeperature of sample}
 Ef:=1.9;              {Fermi-level}
 Ntrap:=6.4E20;        {density of traps}
 writeln('Ntrap= ',Ntrap);
 vphonon:=1.0E0;   {phononfrequency, choosen to be 1,0 in order to get the right time scale}
 evenwicht(start,pvrij0,Nt);                {calculation of equilibrium values}
 dndt(pvrij0,start,Nt);                     {calculation of the amount of trapping at t=i}
 close(f2);
 writeln('the program is ready, press a key to continue');
 repeat until keypressed;
end.
```

Appendix B.

This program is written to be able to study the effects of a conduction current. The difference with the program given in appendix A is that we can alter the amount of distances from one to a user defined number. The calculation of the trapping for every distance is similar to that of appendix A. Furthermore, the program gives as output the current as function of the time by integration over the distance. This program is also written for electron trapping.

```
program traps;
{$N+}
uses printer,crt;

CONST  q= 1.60218E-19;
       h= 6.62617E-34;
       c= 10;
       m0= 9.1095E-31;
       pi= 3.1415927;
       kb= 1.38E-23;
       mu= 0.5E-10;
       np ={100}1000;
       dt= 5.0E-7;
       nstep= {100}1000;
       nafstand= 10;

TYPE   arraytrap     = array [1..c] of real;
       arrayvec      = array [0..nstep] of real;
       arrayafstand  = array [0..nafstand] of real;
       arraynp       = array [1..np] of real;
       matrix        = array [1..nafstand,1..c] of real;

VAR    m,x,t                 : integer;
       Ef,Te,T0,V,L,Ntrap    : real;
       vph,p0                : real;
       Jc                    : arraynp;
       tijd,J                : arrayvec;
       p,dp,dJ               : arrayafstand;
       Nt,tesc,cross         : arraytrap;
       f2                    : text;
       pt0                   : matrix;

procedure evenwicht(VAR pt0:matrix;VAR p0:real;VAR cross,Nt,tesc:arraytrap);
var
 Nc,N,Et   : real;
 j         : integer;
const
 Ec=2.0;

Begin
 Nc:=2*(((2*pi*m0*kb*Te)/(h*h))*sqrt((2*pi*m0*kb*Te)/(h*h)));
 p0:=Nc*exp(-(Ec-Ef)*q/(kb*Te));                    {p0 is constant for all levels}
   for j:=1 to c do                                 {number of traplevels}
    begin
     Et:=2.01-(0.03*j);
     Nt[j]:=Ntrap*exp(-((2.0-Et)*q)/(kb*T0));
     tesc[j]:=1/(vph*exp(-(Ec-Et)*q/(kb*Te)));
     N:=Nc*exp(-(Ec-Et)*q/(kb*Te));
     For x:=1 to nafstand do pt0[x,j]:=Nt[j]/(1+N/p0);   {in steady-state}
     cross[j]:=pt0[x,j]/(tesc[j]*p0*(Nt[j]-pt0[x,j]));   {equal for every x}
```

```
      {tcap[x,j]:=tesc[j]*p0/pt0[x,j];                    {equilibriumcondition}
    end;
end;

procedure dndt(VAR p,dp:arrayafstand; VAR pt0:matrix;cross,Nt,tesc:arraytrap);
var  j      : integer;
     p2     : arraytrap;

begin
  dp[x]:=0;
   for j:=1 to c do
     begin
       p2[j]:=p[x]+(pt0[x,j]/tesc[j]-p[x]*cross[j]*(Nt[j]-pt0[x,j]))*dt;      {diff. Equation}
       dp[x]:=dp[x]+(p2[j]-p[x]);                    {verloren vrije ladingen (getrapped)}
       pt0[x,j]:=pt0[x,j]-(p2[j]-p[x]);              {toename van traplading voor ieder nivo}
     end;
end;
Begin          {mainprogram; calculations are in eV, only the number in eV should be given}
 clrscr;
 tijd[0]:=0;
 for m:=1 to nstep do
    begin
      tijd[m]:=np*dt+tijd[m-1];
      J[m]:=0;
    end;
 assign(f2,'c:\leon\output1.dat');
 rewrite(f2);
 vph:=1E6;                          {begin values,}
 L:=2.0E-7;                         {similar to those}
 T0:=700;                           {given in the first}
 Te:=308;                           {program}
 Ef:=1.80;
 Ntrap:=5.0E22;
 V:=4.0;
 evenwicht(pt0,p0,cross,Nt,tesc);
 p[0]:=1.2*p0; p[1]:=1.2*p0;                {begin perturbation}
 for x:=2 to nafstand do p[x]:=p0;          {begin perturbation}
 for m:=1 to nstep do
  begin
   Jc[m]:=0;
   for t:=1 to np do
   begin
    for x:=1 to nafstand do
     begin
       dJ[x]:=nafstand*q*mu*V/sqr(L)*(p[x]-p[x-1]);   {calculation of conduction current}
       dndt(p,dp,pt0,cross,Nt,tesc);                  {calculation of trapping}
     end;
    for x:=1 to nafstand do
     begin
       p[x]:=p[x]+dp[x]-(dt/q*dJ[x]);          {D.V. for particle conservation,dp is negative}
       p[0]:=p[1];
       if (x>1) and (t=np) then                {calculation of current by integration}
       Jc[m]:=((p[x-1]+p[x])/2)*(L/nafstand)+Jc[m];
     end;
   end;
   writeln(f2,tijd[m],q*mu*V/sqr(L)*Jc[m]);
  end;
 close(f2);
 writeln('the program is ready; press a key to continue');
 repeat until keypressed;
End.
```